Repubblica e Cantone Ticino
Dipartimento del territorio

Acidifying Deposition in Southern Switzerland

Monitoring, maps and trends 1983-2022

Ufficio dell'aria, del clima e delle energie rinnovabili
Sandra Steingruber
Telefono: 091 814 29 30, fax: 091 814 29 79 e e-mail: sandra.steingruber@ti.ch
Bellinzona, 28.6.2023

Content

Abstract

Sulphur and nitrogen oxides from combustion processes and ammonia from agriculture can be transported over long distances, transformed and then loaded on natural ecosystems causing acidification and eutrophication of sensitive ecosystems. Because of its proximity to the emission rich Po Plain and its generally abundant precipitations, Southern Switzerland is particularly exposed to deposition of anthropogenic pollutants.

This reports contains an update of the sulphur, nitrogen and acid deposition maps of the Canton of Ticino for the time periods 1983-1987, 1988-1992, 1993-1997, 1998-2002, 2003-2007, 2008-2012, 2013-2017, published by Steingruber (2018) and the new maps of the period 2018-2022. They were calculated by adding up wet with dry deposition maps. Wet deposition maps were obtained by multiplying precipitation maps with rainwater concentration maps, calculated with multiple linear regression equations describing rainwater concentrations as a function of latitude, longitude and altitude. Dry deposition maps were delivered by Meteotest.

The results show that during the last 30 years average total deposition of sulphur and nitrogen decreased from 114 to 22 meq m^{-2} yr^{-1} and from 158 to 114 meq m^{-2} yr^{-1}, respectively. As a consequence of reduced sulphur and nitrogen deposition, the average present load of acidity decreased from 202 to 96 meq m^{-2} yr^{-1}.

The analysis also showed that most deposition of acidifying compounds occurs through wet deposition (70-79%). As a consequence of the strong decrease in sulphur deposition the relative importance of sulphur compounds in determining total deposition of acidifying compounds has decreased from 43% to 16%, while that of oxidized nitrogen has increased from 29% to 35% and that of reduced nitrogen from 27% to 49%.

Introduction

"Acid rain" is a broad term used to describe the deposition pathway of acidifying compounds from the atmosphere to the surface of the earth. Acidifying deposition has two components: wet and dry. Wet deposition refers to acidifying rain, fog, and snow, while dry deposition refers to acidifying gases and particles. The primary causes of acidifying deposition are the emissions of sulphur dioxide (SO_2) and nitrogen oxides (NO_x) from combustion of fossil fuels as well as ammonia (NH_3) emissions from agriculture. In the atmosphere SO_2 and NO_x can be oxidized to sulphuric and respectively nitric acid causing acid precipitation. Although ammonia itself reacts as a base in the atmosphere (resulting in the formation of ammonium, NH_4), during the assimilation by plants the temporary bound proton is released again to the environment. In addition, in soils and waters ammonium can be oxidized by microorganisms to nitrate (nitrification), releasing two protons. In this way, ammonia emissions can contribute to the acidification of soils and waters.

Acidifying deposition affects the environment in several ways. Acidification of surface waters gradually leads to severe changes in biological communities. Effects range from reductions in diversity without changes in total biomass to elimination of all organisms (Dillon et al. 1984). Damages to forests include weakening of the root system, nutrient imbalances and defoliation. Building materials and works of art can also be damaged by corrosion due to acid deposition. Also health problems, especially respiratory and cardiovascular diseases, have been found to be associated with increased concentrations of particulate matter (i.e. aerosols) and ozone, both formed by precursors such as sulphur oxides, nitrogen oxides, volatile organic compounds and ammonia.

Acidifying deposition first began with the industrial revolution, when large amounts of fossil fuels were burnt to produce steam power needed to drive machinery. The term "acid rain" was coined in the 19th century by the scientist Robert Smith, working at the time in Manchester (Smith 1852). In those times acid rain was confined to industrial towns and cities. However, the situation gradually worsened and widespread environmental damage on a global scale was observed by scientists in the second half of the 20th century.

In the sixties the link between sulphur emissions in continental Europe and acidification of Scandinavian lakes had been demonstrated (Odén 1968). Between 1972 and 1977 several studies confirmed the hypothesis that air pollutants can travel several thousands of kilometers before deposition and damage occur, evidencing that cooperation on an international level was necessary to solve problems such as acidification. As a consequence in 1979 34 Governments, including Switzerland, and the European Community (EC) signed the Convention on Long-range Transboundary Air Pollution (CLRTAP). The Convention entered into force in 1983. Today it has 51 Parties and has been extended by eight specific protocols. Four of these protocols control acidifying pollutants.

The Helsinki Protocol of 1985 aimed at reducing sulphur emissions by at least 30%. The goal of the Sofia Protocol of 1988 was the freezing of the emissions of NO_x. The 1994's Oslo Protocol required further reduction of sulphur emissions and the Gothenburg Protocol of 1999 set national emission ceilings for sulphur, NO_x, VOC's and ammonia for 2010. As a consequence, a substantial reduction in the emissions of sulphur and nitrogen oxides has been achieved over the last 20-25 years (EMEP 2022) leading to an improved quality of atmospheric deposition.

Figure A: Annual sulphur dioxide, nitrogen oxides and ammonia emissions in Switzerland from 1900 to 2030. Dashed lines after 2020 are projections

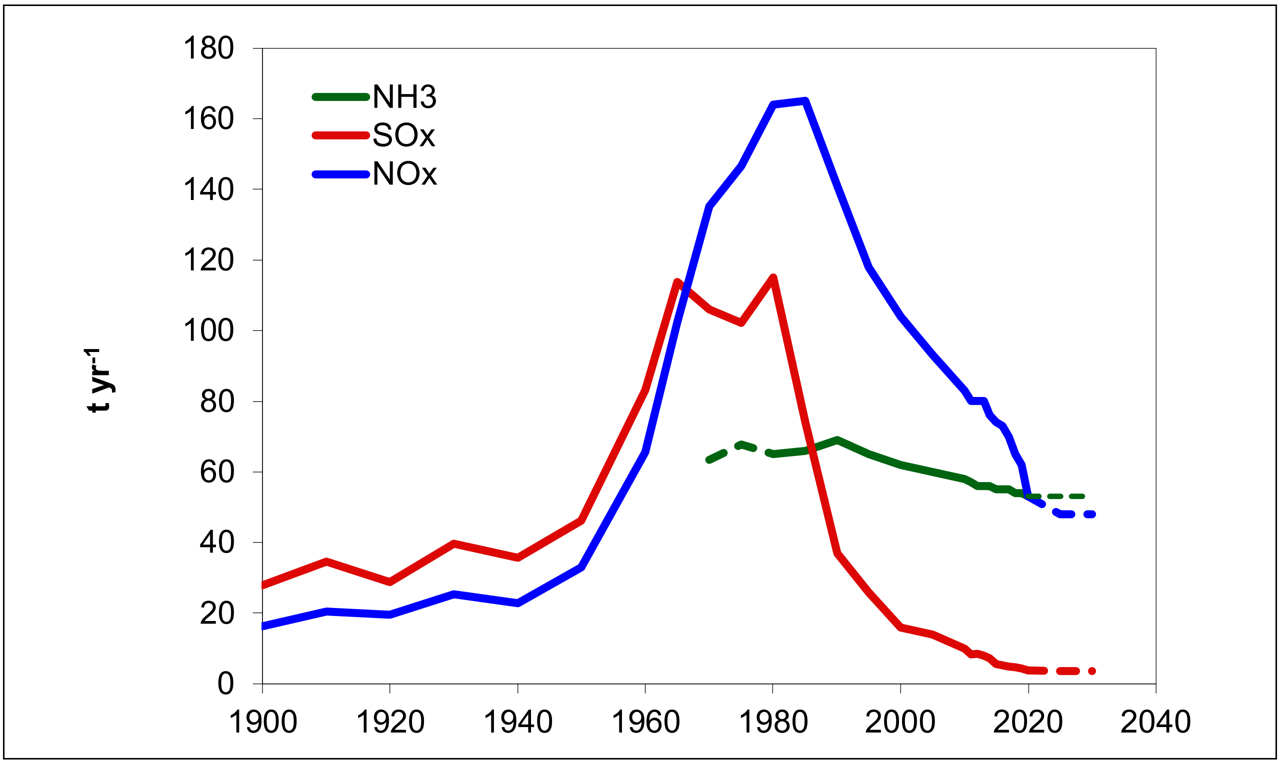

Fig. A shows the emissions of sulphur and nitrogen oxides and ammonia in Switzerland from 1900 to 2030 (Künzler 2005, Bass et al. 2022). The sulphur and nitrogen oxides emissions started to increase steeply after the second world war. Sulphur oxides reached their maximum between 1965 and 1980, while nitrogen oxides peaked around 1985. Afterwards, both sulphur and nitrogen oxides decreased continuously 2020. Ammonia decreased only little. The reduction of sulphur dioxide emissions has mainly been caused by a reduction of the sulphur content in liquid fuels and the partial substitution of sulphur rich coal with other fossil fuels. The decrease of the nitrogen oxides emissions after 1985 has been mainly determined by the equipment of cars with catalytic converters and stationary combustion sources with $DeNO_x$-systems. However, because of its particular topography and meteorology the air quality in Southern Switzerland is not only influenced by local emissions but also by transboundary air pollution originating from the Po Plain and particularly from the heavily polluted urban area of Milan and Turin. In fact, wet deposition in Southern Switzerland is mainly determined by warm, humid air masses originating from the Mediterranean Sea, passing over the Po Plain and colliding with the Alps. Furthermore, high altitude soils and freshwaters of Southern Switzerland are particularly sensitive to acidification because of the dominance of base-poor rocks with low buffering capacity. Recently Steingruber showed that in Switzerland still 25% of the analyzed potentially acid sensitive lakes (52) have autumn acid neutralizing capacities (ANC) below 20 meq m^{-3} and 10% of the same lakes have pH values below 6.0 (Austnes et al. (2018). Compared to the past, the present acidification status has improved. During the large scale survey in 1995, 40% and 29% of the 45 analyzed lakes had autumn ANC and pH values below 20 meq m^{-3} and 6.0, respectively. Decreasing depositions of S have been the main reason for the observed chemical recovery (Rogora et al. 2013). More recently N accounts for about 80% of the acidifying deposition (Rogora et al. 2016), which mean that for a further recovery of the lakes chemistry emissions of N have to be significantly reduced. Austnes et al. (2018) concluded that acidification is still observed in many other countries in Europe and North America, as well and that even by reaching the emission targets of acidifying compounds set for 2030, critical loads for surface waters will remain exceeded. As a consequence, it is important to continue to monitor acidifying deposition, especially at the more sensitive sites. As regards Southern Switzerland, acidifying deposition has already been assessed by Barbieri and Pozzi (2001), Steingruber and Colombo (2010) and Steingruber (2018) for the following time periods: 1983-1987, 1988-1992, 1993-1997, 1998-2002, 2003-2007, 2008-2012, 2013-2017. This report contains the update of the already published 5-years deposition maps by considering the recalculated dry deposition maps of nitrogen (FOEN 2023) and the deposition maps of the last 5-year period (2018-2022). In particular, the aims of this report are:

- to describe the rainwater quality at different sampling stations in Southern Switzerland from 1988 to 2022;
- to calculate temporal trends for the main chemical parameters present in rainwater involved in the process of acidification;
- to map wet deposition of the main chemical parameters for Southern Switzerland for five-years periods from 1983 to 2022 with the aid of multiple regression analysis between concentrations of parameters relevant for acidification and geographic parameters;
- to map total deposition by adding up wet and dry deposition, the latter being modeled by Meteotest.

1. Precipitations in Southern Switzerland

1.1 Introduction

Precipitation volumes influence very much rainwater quality and the amount of wet deposition of air pollutants. For this reason precipitation maps have been calculated in 5-years time periods.

1.2 Sampling sites

For the 2018-2022 map, yearly precipitation from totally 78 pluviometric (68 Swiss, 10 Italian) stations were used to estimate the amount of precipitation over Southern Switzerland (for the maps before 2018, see Steingruber 2018). The Swiss data originated from different precipitation monitoring networks: the Federal Office of Meteorology and Climatology (MeteoSwiss) and the Canton of Ticino with data from Ufficio dei Corsi d'Acqua (UCA). The Italian data were provided by the Regional Agencies for the Protection of the Environment (ARPA) of Lombardy and Piedmont, the national agency for electric energy (ENEL) and the hydroelectric power agencies (Idroelettriche Riunite S.p.A.). The geographic distribution of the precipitation sampling sites is shown in Fig. 1.1. Longitudes, latitudes and altitudes and data source are reported in Tab. A1 of the Appendix. For the maps previous 2018 see Steingruber (2018).

Figure 1.1: Precipitation sampling sites used for the period 2018-2022

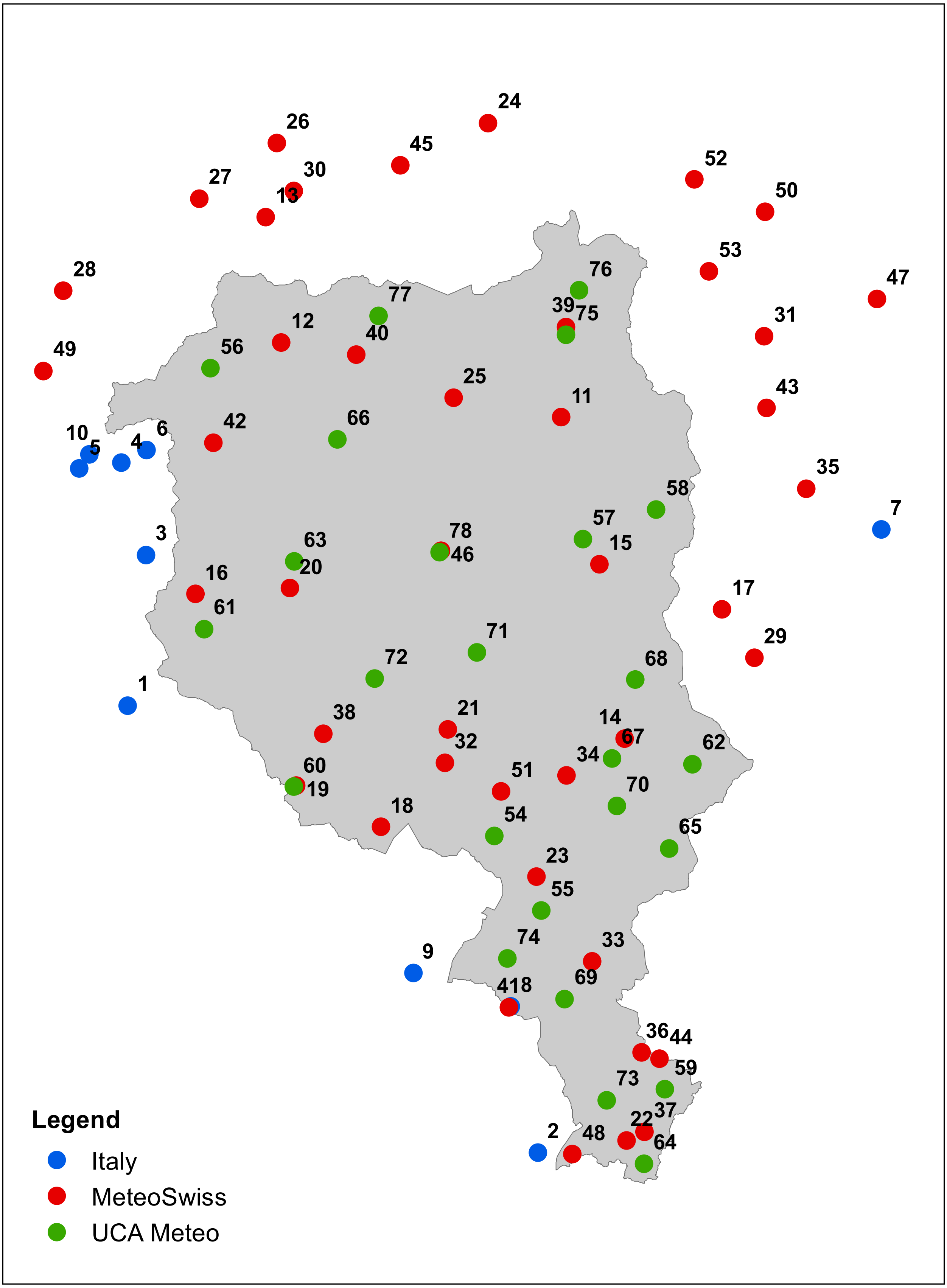

1.3 Mapping method

Existing national precipitation maps were refined for the study area with the following procedure: 5-years precipitation means were calculated for each precipitation sampling site and divided by the values extracted from the national precipitation maps (resolution: 1km x 1km) provided by MeteoSwiss.

The resulting factors were interpolated by the inverse distance weighting method in ArcGIS® (registered trademark of Esri Inc., Redlands, USA) using the following parameters: distance exponent = 2, number of points = 3, maximal search distance = 11 km, resolution = 1 km x 1km. These maps were then multiplied back by the precipitation maps.

1.4 Precipitation maps

The calculated precipitation maps are shown in Fig. 1.2. Mean annual precipitation was 1903 mm in 1983-1987, 1667 mm in 1988-1992, 1873 mm in 1993-1997, 2038 mm in 1998-2002, 1313 mm in 2003-2007, 1880 mm in 2008-2012, 1815 mm in 2013-2017 and 1631 in 2018-2022. Interestingly, 1998-2002 was one of the wettest and 2003-2007 one of the driest 5-year period ever measured. The wettest region is situated in the western part of the study area. This region includes the Centovalli's, the Onsernone's and the lower Maggia's valley. The reasons for this distribution are air masses rich in humidity moving predominantly from southwest toward the Southern Alps and the particular orography of the area causing a steep raise of the air masses to higher altitudes. Other rain rich regions are located in the northwestern part (higher Maggia valley), in the north-central part (higher Verzasca valley) and in the center of the Canton of Ticino (mount Tamaro-Gradiccioli). Precipitation is lowest in the eastern part of the Canton due to less frequent exposure to humid currents. For a more detailed description of the climate in the studied area one may refer to Spinedi and Isotta (2004) and MeteoSvizzera (2012).

Figure 1.2: Precipitation maps: 1983-1987, 1988-1992, 1993-1997, 1998-2002, 2003-2007, 2008-2012, 2013-2017, 2018-2022

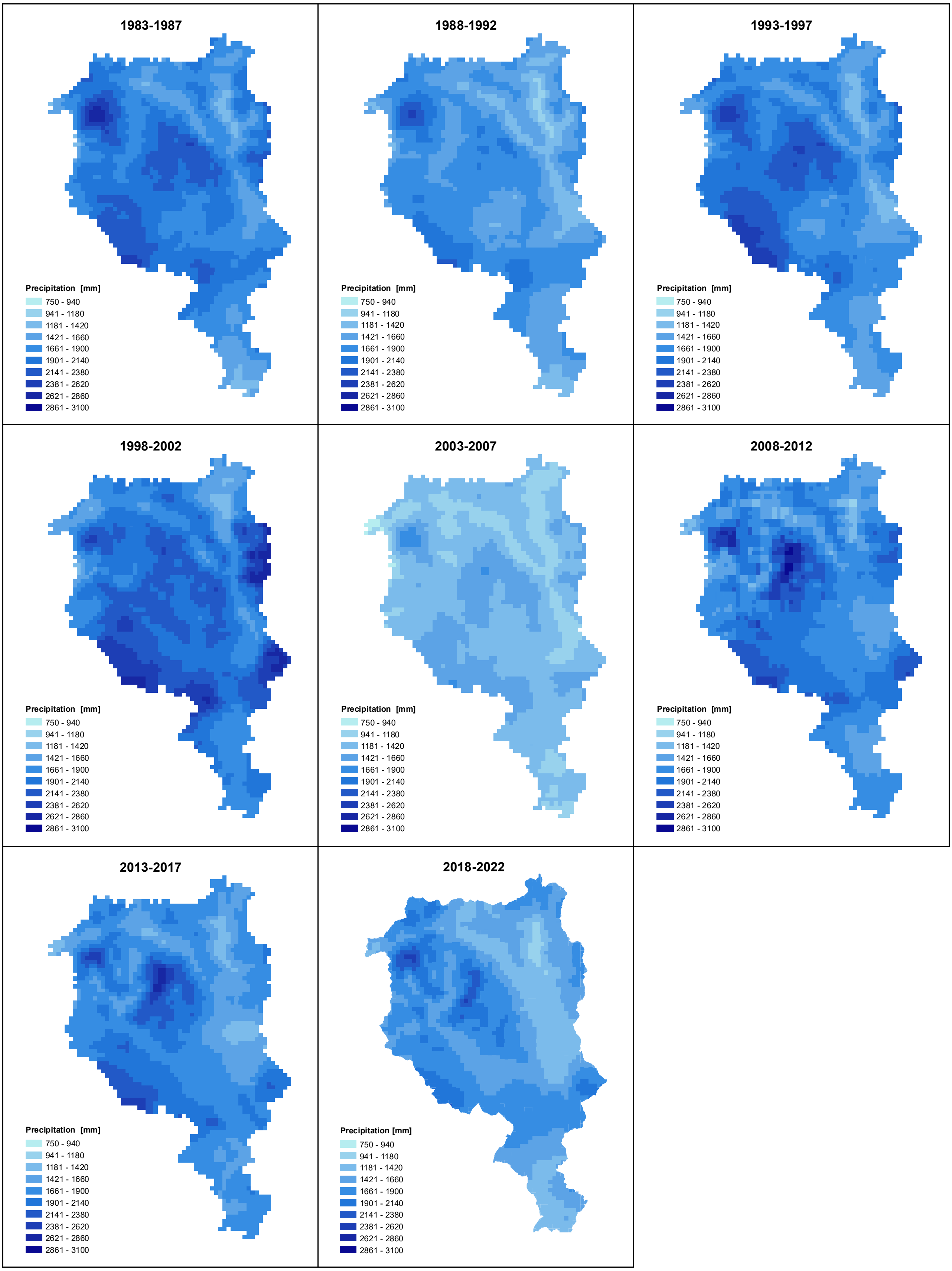

2. Rainwater quality

2.1 Sampling sites

Sampling of wet deposition was carried out at weekly intervals. Between 1982 and 1985 rainwater was collected at Locarno Monti and Lugano with bulk samplers. Since 1988, wet-only samplers have been used. Sampling of wet deposition started at Acquarossa, Piotta and Stabio in 1990, at Monte Bré in 1995, at Robiei in 1996, at Bignasco and Sonogno in 2001 and at the Cristallina hut in 2017. Precipitation at the Cristallina hut occurs only during the months when the hut is inhabited by the guardian (about 9 months per year). Sampling sites were chosen along a south-north axis and at various altitudes (200-2572 m a.s.l.). In order to better describe the dependence on geography, results from the closed-by Italian sampling sites were included in the statistical analysis (data have been provided by the Institute of Ecosystem Study in Pallanza, Italy). In addition, to facilitate the modeling of rainwater concentrations at very high altitudes, results from the analysis of snow sampled at the Basodino glacier (2650-3100 m) were also considered. Snow cores representing the snow fallen between October and May were sampled almost every spring since 1993. From these “winter” concentrations, yearly concentrations were calculated by the multiplication with the year to winter concentration ratios measured at the nearby site Robiei.

The geographic distribution of the sampling sites used for the 2018-2022 maps and their geographic coordinates are shown in Fig. 2.1 and Tab. 2.1, respectively. Compared to the analysis prior 2018, the Italian sampling sites decreased in number (see Steingruber 2018).

Figure 2.1: Study area with wet deposition sampling points during the period 2018-2022

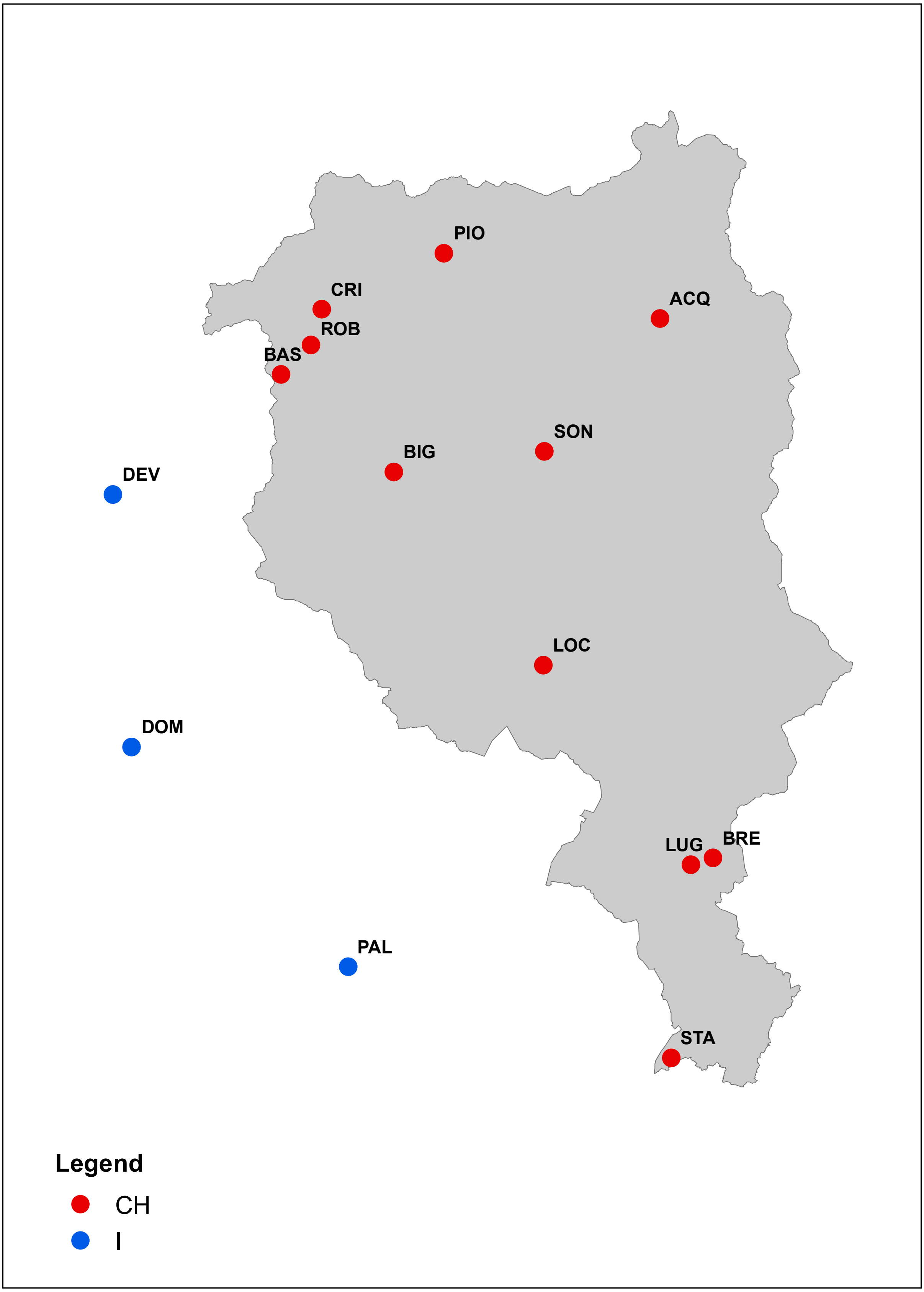

Table 2.1: Swiss (CH) and Italian (I) wet deposition sampling sites and their geographic (WGS84) and Swiss (CH1903 LV03) coordinates, altitudes and sampling years

Acronym	Sampling site	WGS84		CH1903 LV03 (m)		Altitude (m a.s.l.)	Sampling years
		North	East	North	East		
ACQ	Acquarossa	46°27'41''	8°56'12''	146440	714998	575	1990-1991, 1993-2022
BIG	Bignasco	46°21'11''	8°36'41''	132257	690205	443	2001-2022
LOC	Locarno Monti	46°10'27''	8°47'17''	114350	704160	367	1982-1985, 1988-1991, 1993-2022
LUG	Lugano	46°00'24''	8°57'18''	95870	717880	273	1982-1985, 1989-1991, 1993-2022
BRE	Monte Brè	46°00'32''	8°59'17''	96470	719900	925	1995-2022
PIO	Piotta	46°31'07''	8°40'35''	152500	694930	1007	1990-1991, 1993-2022
ROB	Robiei	46°26'43''	8°30'51''	143984	682540	1890	1996-2022
SON	Sonogno	46°21'05''	8°47'14''	134150	704250	918	2001-2022
STA	Stabio	45°51'36''	8°55'52''	77970	716040	353	1990-1991, 1993-2022
DEV	Devero	46°19'19"	8°16'29"	130156	664132	1634	1996-2022
DOM	Domodossola	46°06'42"	8°17'41"	106767	665875	270	1986-2022
PAL	Pallanza	45°55'42"	8°34'48"	86386	686003	208	1985-2017, 1983-2022 (bulk)
BAS	Basodino glacier	46°25'04''	8°28'34''	141000-141500	679500-680000	2650-3100	1993-2003, 2006-2018, 2019, 2021

2.2 Analytics

Rain samples were analyzed for pH, Gran alkalinity, conductivity and the main cations and anions. Parameters, analytical methods and quantification limits are shown in Tab. 2.2.

Table 2.2: Measured parameters, analytical methods, accuracy and quantification limits

Parameter	Acronym	Filtration	Conservation	Methods	Accuracy
pH	pH	No	No	potentiometry	0.02
conductivity	Cond	No	No	Kolrausch bridge (20°C)	1.0 µS cm^{-1}
alkalinity	GranAlk	No	No	potentiometric Gran titration	0.001 meq l^{-1}
					Quantification limit
Ca^{2+}	Ca	CA filter	PP bottle, 4°C	ion chromatography	0.06 mg l^{-1}
Mg^{2+}	Mg	CA filter	PP bottle, 4°C	ion chromatography	0.01 mg l^{-1}
Na^{+}	Na	CA filter	PP bottle, 4°C	ion chromatography	0.01 mg l^{-1}
K^{+}	K	CA filter	PP bottle, 4°C	ion chromatography	0.08 mg l^{-1}
NH^{4+}	NH_4	CA filter	PP bottle, 4°C	ion chromatography	0.03 mg N l^{-1}
SO_4^{2-}	SO_4	CA filter	PP bottle, 4°C	ion chromatography	0.08 mg l^{-1}
NO_3^{-}	NO_3	CA filter	PP bottle, 4°C	ion chromatography	0.02 mg N $^{l-1}$
Cl^{-}	Cl	CA filter	PP bottle, 4°C	ion chromatography	0.1 mg l^{-1}

The quality of the data was assured by regular participation to national and international intercalibration tests. In addition, data were accepted only if the calculation of the ionic balance and the comparison between the measured and the calculated conductivity corresponded to the quality requests included in the programme manual of ICP Waters (ICP waters Programme Centre 2010).

2.3 Concentrations of chemical parameters in rainwater

Fig. 2.2 shows the yearly average concentrations of the main chemical parameters measured in precipitation sampled at the 9 Swiss sampling sites Acquarossa, Bignasco, Monte Brè, Locarno Monti, Lugano, Piotta, Robiei and Sonogno between 1988 and 2022. The concentrations of the last 5 years are tabulated in Tab. A2 of the Appendix. The yearly mean concentrations of the 5-years periods were calculated by weighting weekly concentrations with the sampled precipitation volume:

$$C(X)_a = \frac{\sum_w P_w \cdot C(X)_w}{P_a}$$ where

P_w = weekly precipitation volume (measured with the wet-only sampler)

$C(X)_w$= weekly concentration of compound X

P_a = annual precipitation volume calculated as sum of P_w

Unfortuantely, between 2015 and 2022 the concentrations and depositions of nitrate at Robiei were occasionally influenced by the emission of a generator close to the sampling site. For this reason the concentration of nitrate at Robiei without the local emissions were estimated from the nearby Italian sampling site Devero (distance = 23 km, DEV) provided by the Institute of Ecosystem Study (Verbania Pallanza, Italy). For the same reason GranAlk at Robiei were approximated with ANC by subtracting the sum of the acid anions SO_4, NO_3, Cl from the base cations Ca, Mg, Na and K plus NH_4, while pH values without the influence of the local NO_x emissions could not be reconstructed.

In general, ion concentrations of anthropogenic origin (sulphate, nitrate, ammonia) still decrease with increasing latitude and altitude. The gradients, however, are not as pronounced as they were at the beginning of the measurements. The correlation with latitude and altitude reflects the influence of long-range transboundary air pollution moving along a south to north gradient from the Po plain toward the Alps and the distance from pollution sources.

In addition to the temporal trends that are analyzed and discussed in chapter 2.4, it can be observed that concentrations can vary very much from one year to the other. Because of dilution, during wet years concentrations of sulphate, nitrate and ammonium tend to be lower and during dry years higher than average. It also can happen that single particularly intense rain events with alkaline characteristics can heavily influence yearly mean base cation concentrations and acidity. Exceptionally high base cations and low acidity peaks can be observed at sampling stations Acquarossa, Locarno Monti and Piotta in 2000 (alkaline event in October) and at Monte Bré, Locarno Monti, Lugano and Stabio in 2002 (alkaline event in November). Both events have led to floods in the region. When and why such events appear is still not clear. The sulphate and base cations peaks at Lugano in 2010 were the consequence of the volcanic eruption at Eyafjellajokull (Iceland) in April 2010. Moreover due to the COVID-19 pandemic and the dramatic restrictions on socio-economic activity that caused a reduction of the emissions (EMEP 2022), during 2020 at most sites the concentrations of sulphate, and nitrate were significantly lower than usual (Rogora et al. 2022). Concentrations of ammonium peaked during the warm and dry 2022, mainly during the summer months (Steingruber 2023). Seitler and Meier (2022) noticed that in warm years the gasous ammonia concentrations are generally higher. It is possible that the high summer temperatures during 2022 increased the evaporation rates of ammonia from agriculture. In addition, because of the simultaneous low precipitation at the southern side of the Alps, the long range transport of ammonia/ammonium from the Po Plain may have been facilitated.

Figure 2.2: Mean annual concentrations in wet deposition at the sampling sites

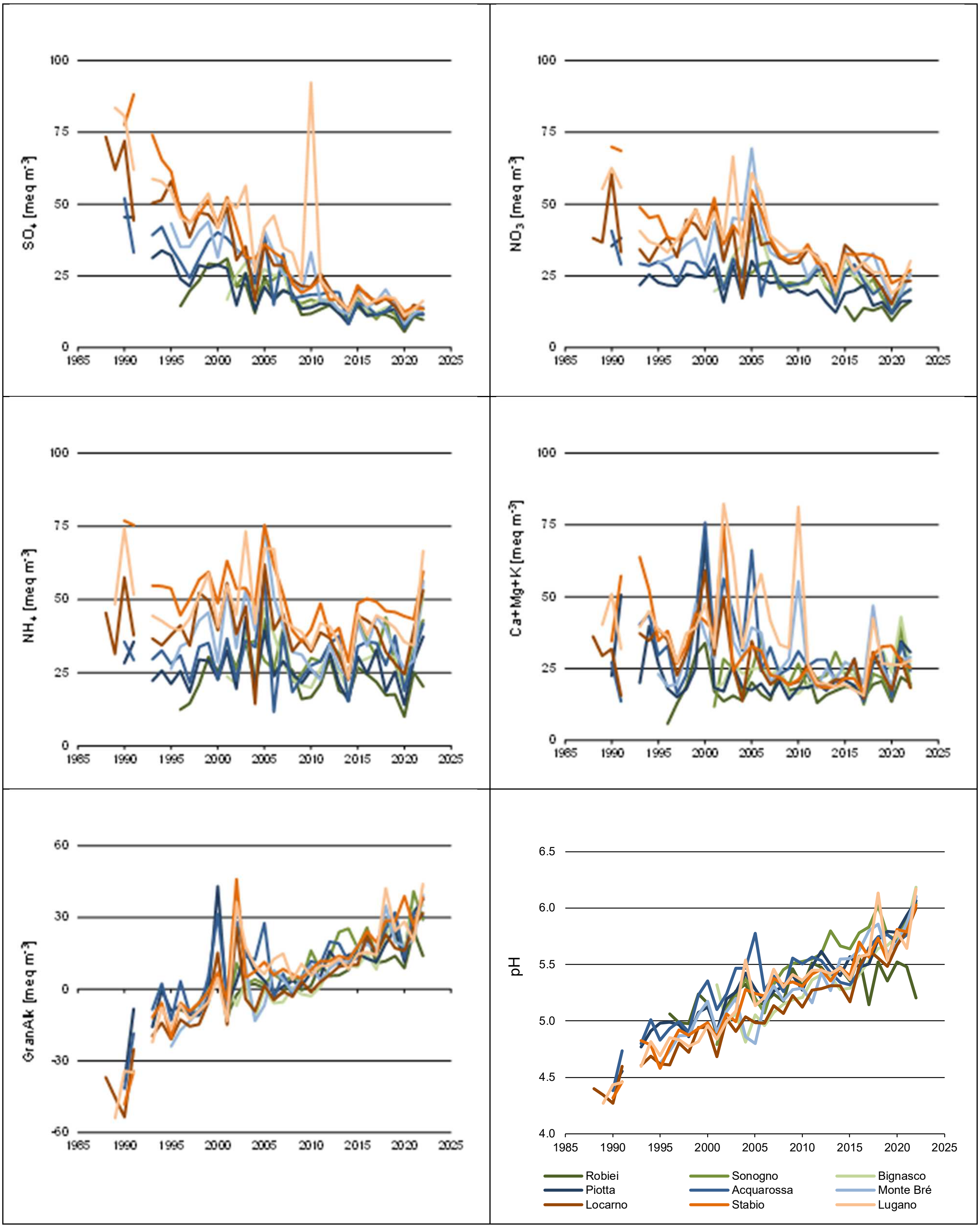

2.4 Trends in rainwater quality

2.4.1 Statistical methods

Trend analyses were performed on the key variables involved in acidification: sulphate, nitrate, ammonium, base cations (calcium, magnesium and potassium), hydrogen ion and Gran alkalinity. For each site and each parameter the monthly mean concentrations weighted with the precipitation volume were calculated and temporal trends were tested with the seasonal Mann-Kendall test (Hirsch et al. 1982) with a correction among blocks (Hirsch and Slack 1984). The two sided tests for the null hypothesis that no trend is present were rejected for p-values below 0.05. Estimates for temporal variations in rainwater quality were quantified with the seasonal Kendall slope estimator (Gilbert 1987). All trend analysis were calculated with the CRAN package “rkt 1.3” (Marchetto 2014).

2.4.2 Results from trend analysis

Trends of rainwater concentrations were analysed for four different time periods: from the beginning of the measurements until 2022, from 1988-1991 until 2000, from 2000 until 2010, and from 2010 until 2022 (Tab. 3.3). Since trends of depositions are “disturbed” by the precipitation volumes that vary irregularly through time, trends in depositions were calculated only for the entire monitoring period in order to level out as much as possible the influence of rainwater volume.

Sulphate concentrations decreased significantly at all sites. The highest change in concentrations occurred at the most polluted sites Locarno Monti, Lugano and Stabio and during the first two analysed time periods (from 1988-1991 until 2000 and from 2000 until 2010). After 2010 concentrations of sulphate still decreased significantly at all sites but much less. Concentrations of nitrate decreased also significantly at all sites particularly between 2000 and 2010 and less after 2010. Concentrations of ammonium decreased significantly at five sites and mainly between 2000 and 2010. The sum of calcium, magnesium and potassium also decreased significantly at five sites and for most of them mainly during 2000-2010. Concentrations of the hydrogen ions decreased significantly at all sites, particularly at the beginning of the monitoring period (1980/1990-2000), but even after 2010 concentrations decreased significantly at most sites although less dramatically. The concentrations of Gran alkalinity increased significantly at all sites during the entire monitoring period.

Table 2.3 Changes in rainwater concentrations (in meq m^{-3} yr^{-1}) during the indicated time periods.
Red rates indicate significant trends

CONCENTRATIONS (meq m^{-3} yr^{-1})	Period	SO_4 beginning-2022	NO_3 beginning-2022	NH_4 beginning-2022	Ca+Mg+K beginning-2022	H beginning-2022	GranAlk beginning-2022
ACQ	1990-2022	-1.11	-0.55	-0.17	-0.61	-0.32	1.26
BIG	2001-2022	-0.60	-0.59	0.02	0.05	-0.43	1.75
BRE	1995-2022	-1.12	-0.59	-0.12	-0.05	-0.48	1.92
LOC	1988-2022	-1.67	-0.85	-0.40	-0.44	-0.94	2.12
LUG	1989-2022	-1.77	-0.80	-0.33	-0.66	-0.58	1.91
PIO	1990-2022	-0.71	-0.51	-0.12	-0.26	-0.46	1.24
ROB	1996-2022	-0.56	-0.36	-0.22	-0.08		0.84
SON	2001-2022	-0.57	-0.45	0.01	-0.17	-0.20	1.23
STA	1990-2022	-1.76	-0.81	-0.32	-0.53	-0.48	2.00

CONCENTRATIONS	Period	SO_4			NO_3			NH_4			Ca+Mg+K			H			GranAlk		
(meq m^{-3} yr^{-1})		'80/'90-00	00-10	10-22	'80/'90-00	00-10	10-22	'80/'90-00	00-10	10-22	'80/'90-00	00-10	10-22	80/90-00	00-10	10-22	80/90-00	00-10	10-22
ACQ	1990-2022	-1.41	-2.14	-0.64	-1.04	-0.76	-0.61	-1.05	-0.93	0.10	-0.47	-2.09	-0.81	-2.29	-0.06	-0.15	4.61	-0.42	1.12
BIG	2001-2022		-1.27	-0.28		-1.19	-0.60		-1.20	0.34		-0.44	0.43		-0.56	-0.28		0.42	2.02
BRE	1995-2022		-1.65	-0.44		-0.63	-0.56		-0.77	0.56		-0.65	0.52		-0.48	-0.20		1.96	2.17
LOC	1988-2022	-2.40	-2.46	-0.69	-0.71	-1.58	-1.22	-0.53	-1.50	0.03	-0.62	-1.25	-0.18	-3.48	-0.76	-0.25	2.56	0.98	1.94
LUG	1989-2022	-2.78	-3.07	-0.58	-1.22	-1.47	-0.49	-0.11	-1.69	0.68	0.09	-1.61	0.14	-2.85	-0.42	-0.11	3.76	1.39	1.27
PIO	1990-2022	-1.43	-1.01	-0.21	-0.62	-0.58	-0.49	-0.11	-0.70	0.22	-0.87	-0.89	0.65	-1.63	-0.31	-0.24	2.43	0.10	1.86
ROB	1996-2022		-1.17	-0.23		-0.43	-0.50		-0.77	-0.17		-0.48	0.19		-0.28			0.44	0.55
SON	2001-2022		-1.14	-0.40		-0.66	-0.61		-0.88	-0.07		-0.65	-0.21		-0.42	-0.08		0.57	0.80
STA	1990-2022	-3.44	-2.48	-0.51	-2.07	-1,11	-0.32	-0.85	-1.32	0.91	-2.17	-1.38	0.49	-2.65	-0.47	-0.08	4.30	1.72	1.92

2.5 Multiple regression analysis

In former reports it has been shown that the geographic distribution of the concentrations of sulphate, nitrate, ammonium and base cations in rainwater of Southern Switzerland can be described with a multiple linear regression model with the variables latitude, longitude and altitude (Barbieri and Pozzi 2001, Steingruber and Colombo 2010, Steingruber 2018).

For this purpose for the Swiss and Italian sampling sites (Tab. 2.1), we calculated the 5-years mean concentrations of sulphate, nitrate, ammonium and base cations weighted with the precipitation volume for the period 2018-2022. The so obtained mean concentrations are reported in Tab. A3 of the Appendix.

Multiple linear regression analyses were then performed for sulphate, nitrate, ammonium and base cations. Parameters for the following multiple linear regressions were derived:

$C = m_{long}*longitude + m_{lat}*latitude + m_{alt}*altitude + C_0$

where:

C = mean concentration weighted with the amount of precipitation over the studied time period

C_0 = intercept

m_{lat}, m_{long}, m_{alt} = linear regression coefficients (=slopes)

Longitude, latitude and altitude are given in m (Swiss projection CH1903 LV03).

The linear regression coefficients for sulphate, nitrate, ammonium, base cations and the values describing the statistic significance of the regression model are reported in Tab. A4 of the Appendix. Concentrations of sulphate and nitrate depended significantly on latitude, longitude and altitude, concentrations of ammonium on latitude and concentrations of base cations on longitude and altitude

.

3. Wet deposition

3.1 Geographic interpolation

The multiple parameter regression model described in the previous chapter permitted the calculation of concentrations maps. The area under investigation was divided into 1km x 1km cells. For every cell center, a concentration of the chemical parameter for the corresponding longitude, latitude and altitude was calculated.

Wet deposition maps of sulphate, nitrate, ammonium and base cations were obtained by multiplying concentration maps with precipitation maps.

3.2 Maps

The wet deposition maps of sulphate, nitrate, ammonium and base cations are shown in Fig. 3.1-3.4 . For comparison not only the most recent 2018-2022 maps were shown but also those of the previous 5 years periods.

The maps show well how wet deposition changed with time. A significant decrease in deposition of especially sulphate but also of nitrate and ammonium can be observed. Wet deposition of base cations also decreased slightly with time. Particularly rain rich and rain poor years can have visible consequences on deposition. As an example deposition of nitrate, ammonium and base cations were slightly higher during the rain rich 1998-2002 period compared to the immediately previous and successive time periods.

Figure 3.1: Wet deposition of sulphate

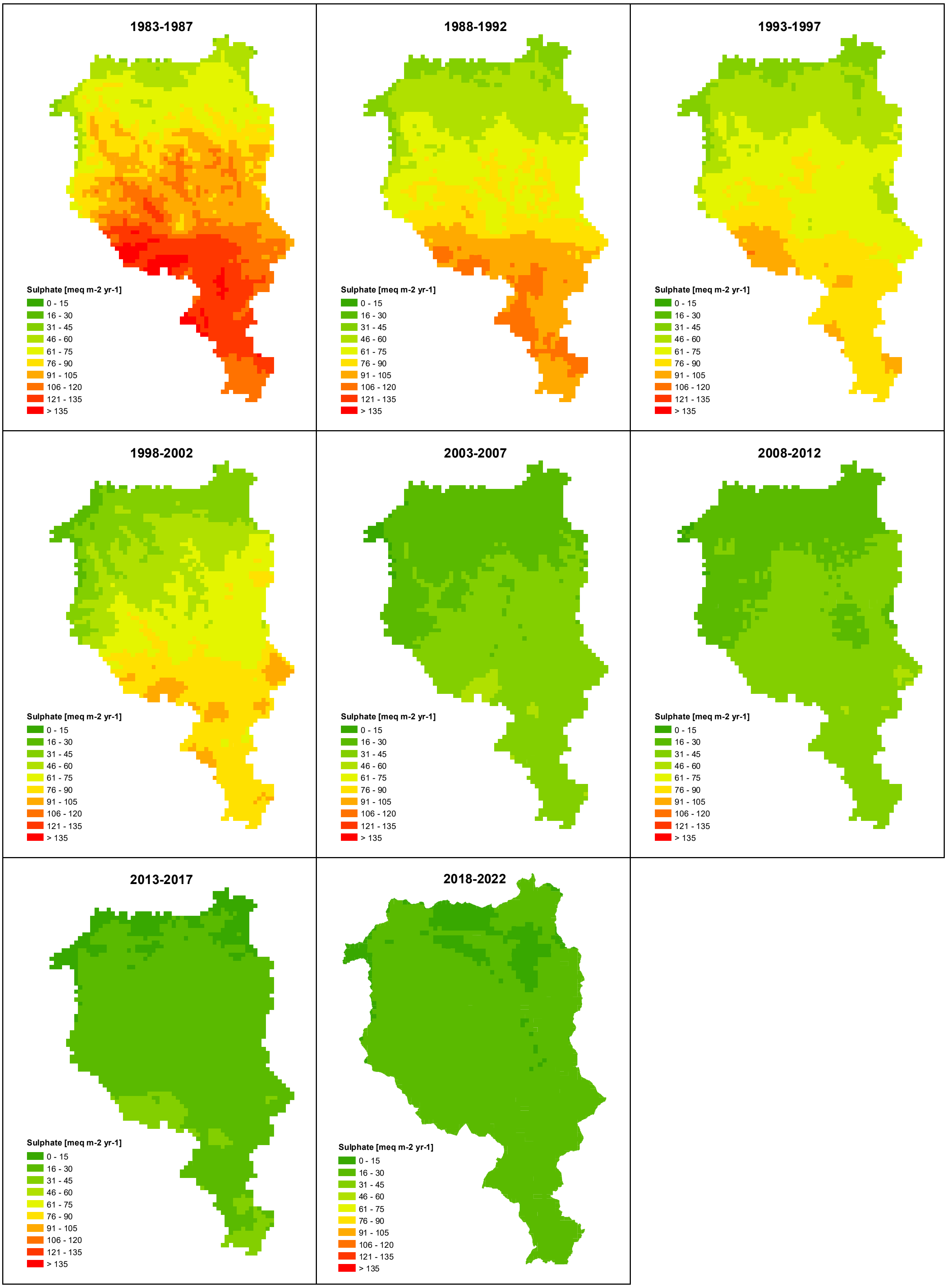

Figure 3.2: Wet deposition of nitrate

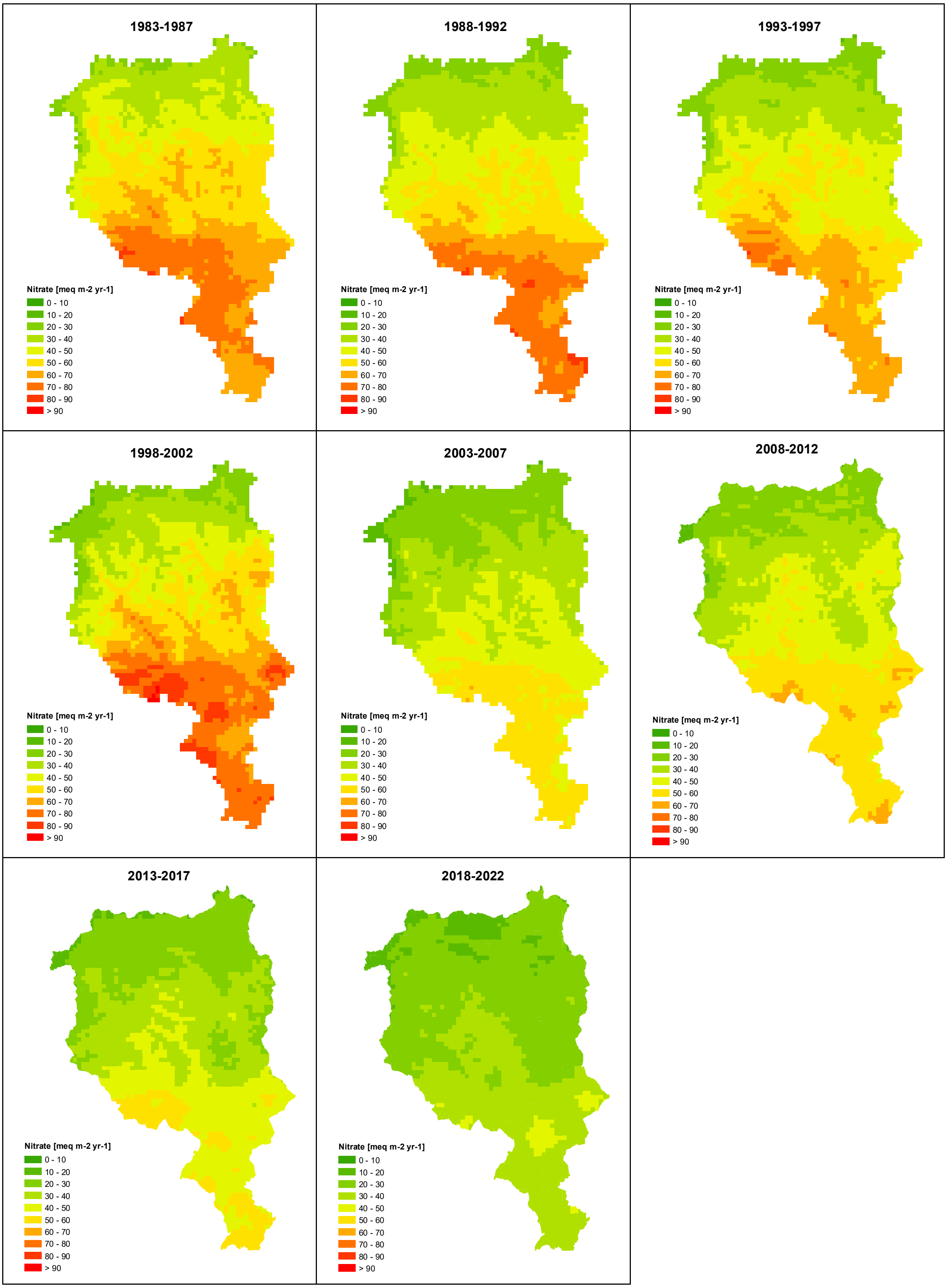

Figure 3.3: Wet deposition of ammonium

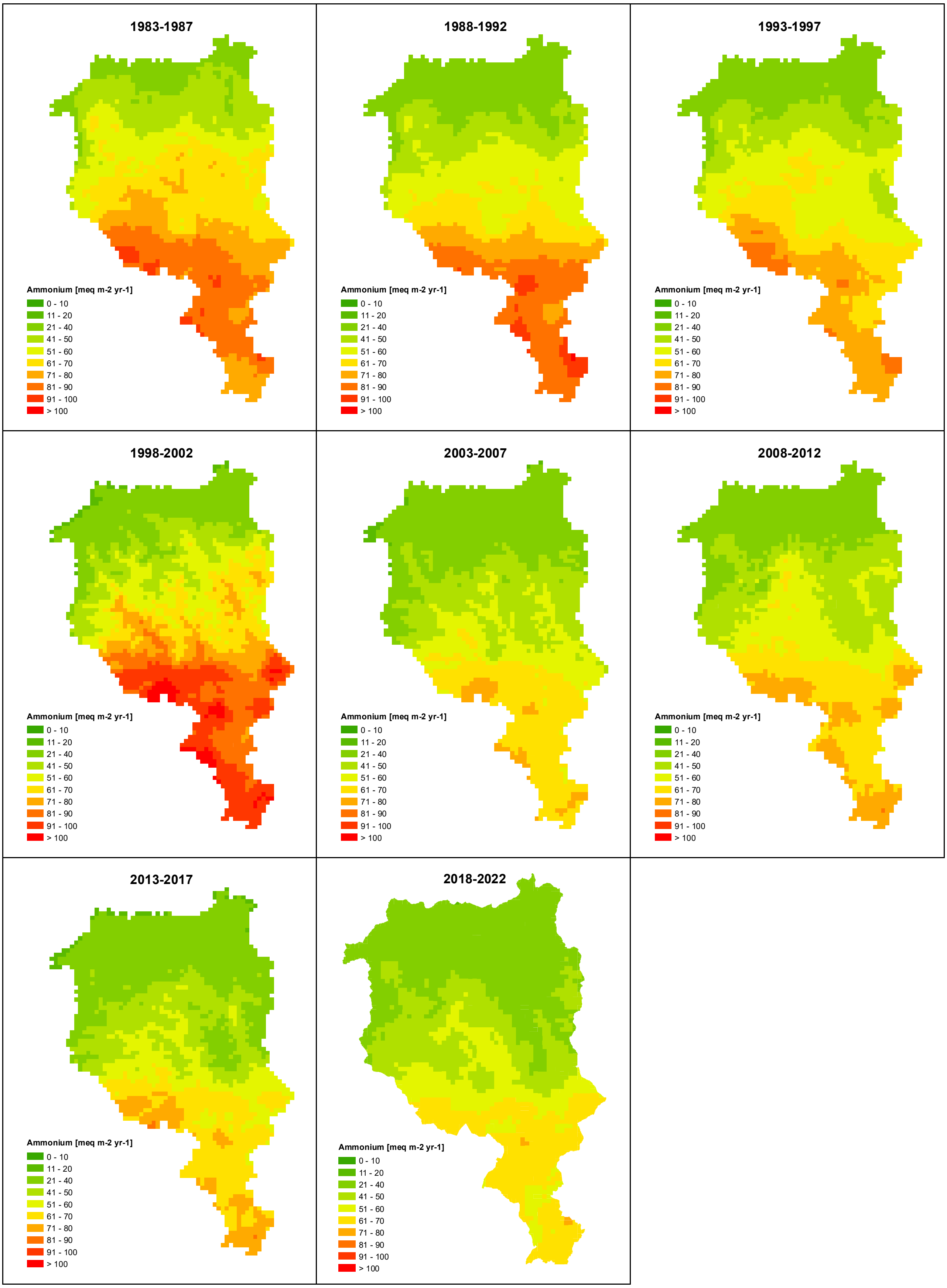

Figure 3.4: Wet deposition of base cations (Ca+Mg+K)

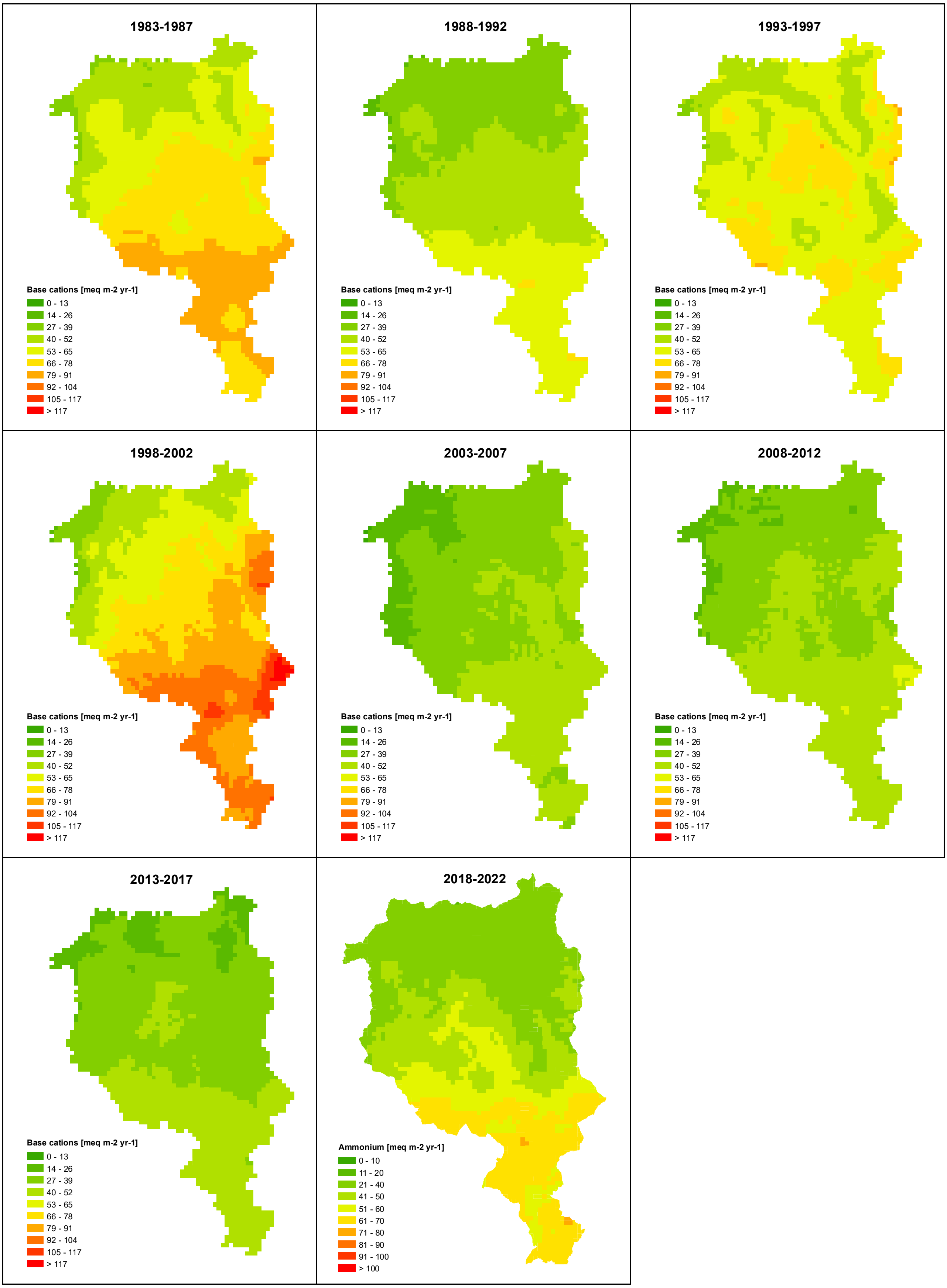

4. Dry deposition

4.1 Mapping methods

Besides wet deposition, dry deposition of gases and aerosols also contribute to total deposition. For quantifying total acidifying deposition, dry deposition of the gaseous compounds NH_3, NO_2, SO_2 , HNO_3 and of the NH_4^+- and NO_3^--containing aerosols has to be known. Dry deposition of sulphate is not considered since its values are negligible compared with those of wet deposition (Hertz and Bucher 1990). SO_2 and NO_x are emitted from combustion of fossil fuels, HNO_3 is formed by photochemical oxidation of NO_2, while NH_3 is mainly emitted from livestock breeding and from use of mineral fertilizers.

Unlike wet deposition, dry deposition cannot be measured directly. Therefore, yearly dry deposition maps are calculated by Meteotest on behalf of the Federal Office for the Environment multiplying modelled air concentrations (annual means, see https://www.bafu.admin.ch/bafu/en/home/topics/air/state/data/historical-data/maps-of-annual-values.html, Künzle 2022) with average deposition velocities (FOEFL 1994, FOEN 2023). Meteotest provided S and N maps for period 2018-2021 and updated N maps for the periods 1988-1992, 1998-2002, 2003-2007, 2008-2012 and 2013-2017. Due to lacking data, dry depositions of the period 1993-1997 were calculated by averaging values of 1988-1992 and 1998-2002.

Since there is almost no measurement for dry depositions of non-marine base cations, values modelled by EMEP for the year 2000 were used for the calculations. Wet and dry deposition values of calcium, magnesium and potassium of the 3 main 50km x 50km grid falling in Canton Ticino (EMEP i,j: 70, 38; 71, 37; 71, 38) were used to calculate their ratio. Afterwards, wet deposition maps of base cations were divided by the average wet to dry deposition ratio (=14) to create dry deposition maps of base cations.

4.2 Maps

Dry depositions of SO_2, oxidized and reduced nitrogen and base cations are mapped in Fig. 4.1-4.4. As a result of reduced emissions, dry deposition of SO_2 and oxidized nitrogen decreased during the last 35 years. Differently, dry deposition of reduced nitrogen was highest during 2018-2021. This is partially due to the introduction of a correction factor from 2018 to better describe the situation in Southern Switzerland (the models before 2018 slightly underestimated the deposition of reduced N), but also to indeed higher mean dry deposition values of reduced nitrogen during 2018-2021 (FOEN 2023). In fact, Seitler and Meier (2022) reported for the years 2018 to 2020 the highest ammonia concentrations in Switzerland ever measured since the beginning of the measurements in 2000 and noticed that in warm years the ammonia concentrations are generally higher. A possible reason might be an increase of the emissions from animal husbandry with increasing temperature (FOEN 2023). A second reason for the general increase of gaseous ammonia that occurs despite the introduction of federal and cantonal measures to reduce the emissions, may be the increase of the gaseous ammonia vs. aerosol ammonium ratio, caused by the decrease of sulfuric and nitric acid (Grange et al. submitted). In fact, the latter are responsible for the transformation of ammonia into ammonium (wet and dry).

Figure 4.1: Deposition of sulphur dioxide

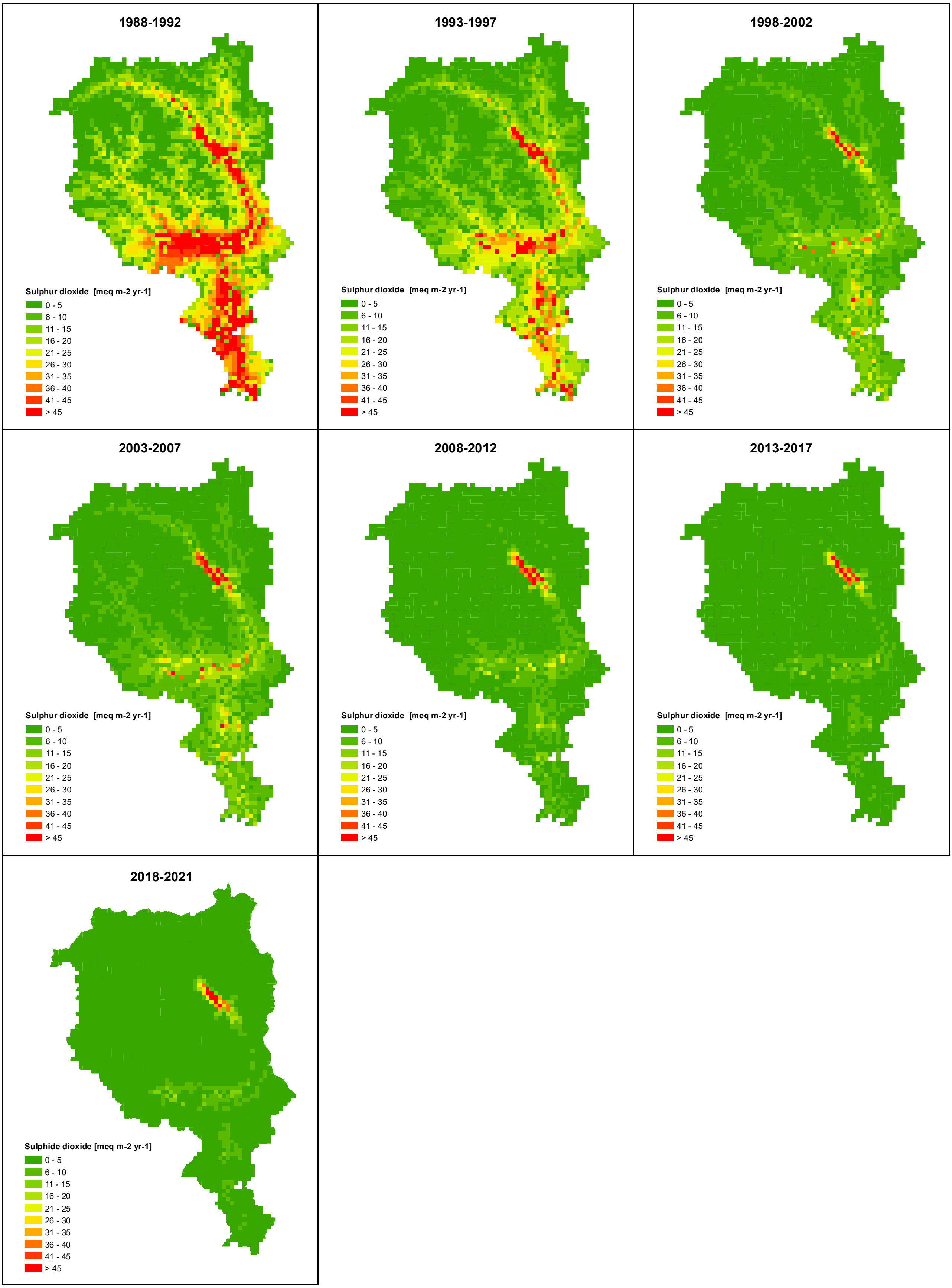

Figure 4.2: Dry deposition of oxidized nitrogen

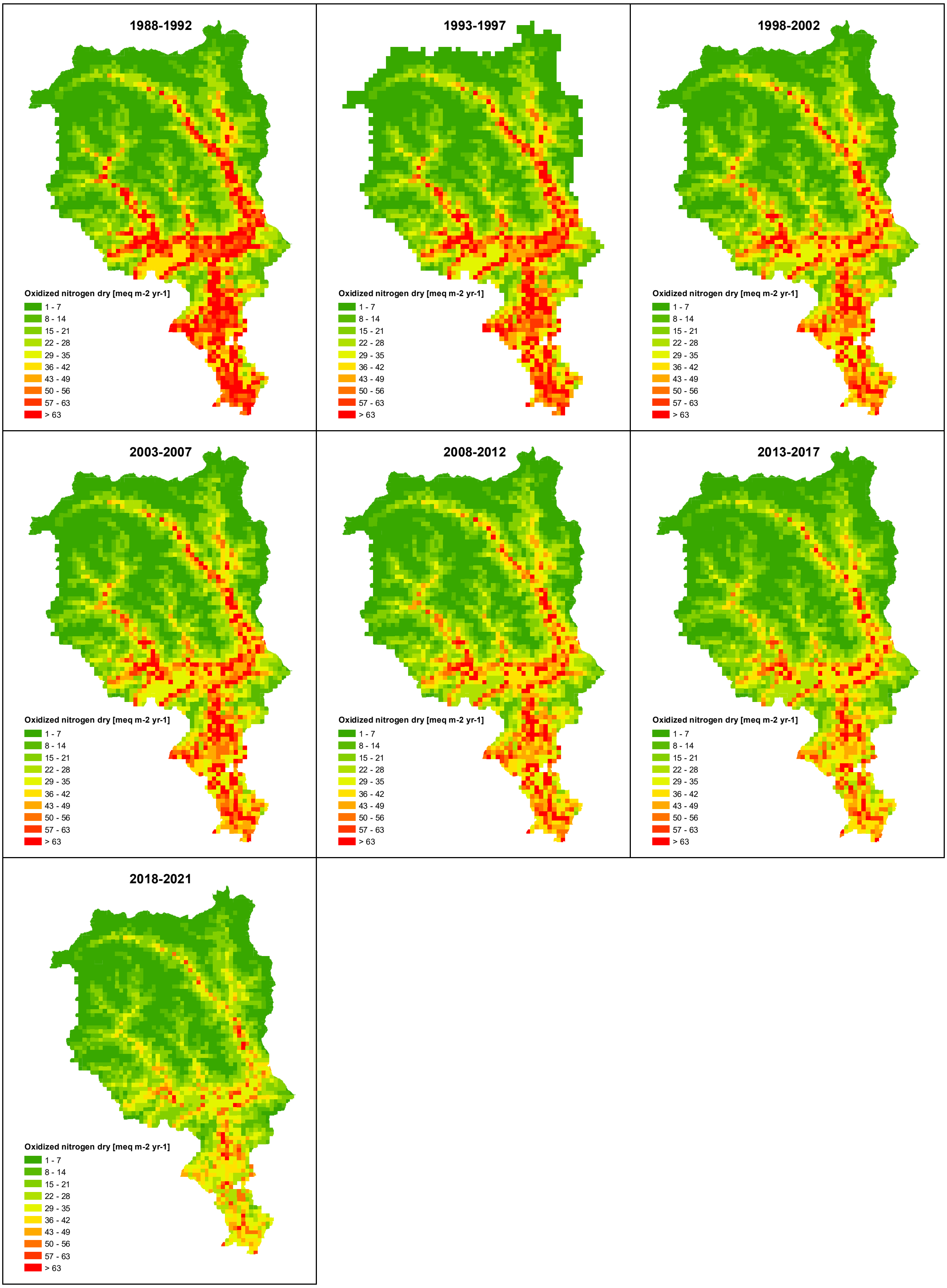

Figure 4.3: Dry deposition of reduced nitrogen

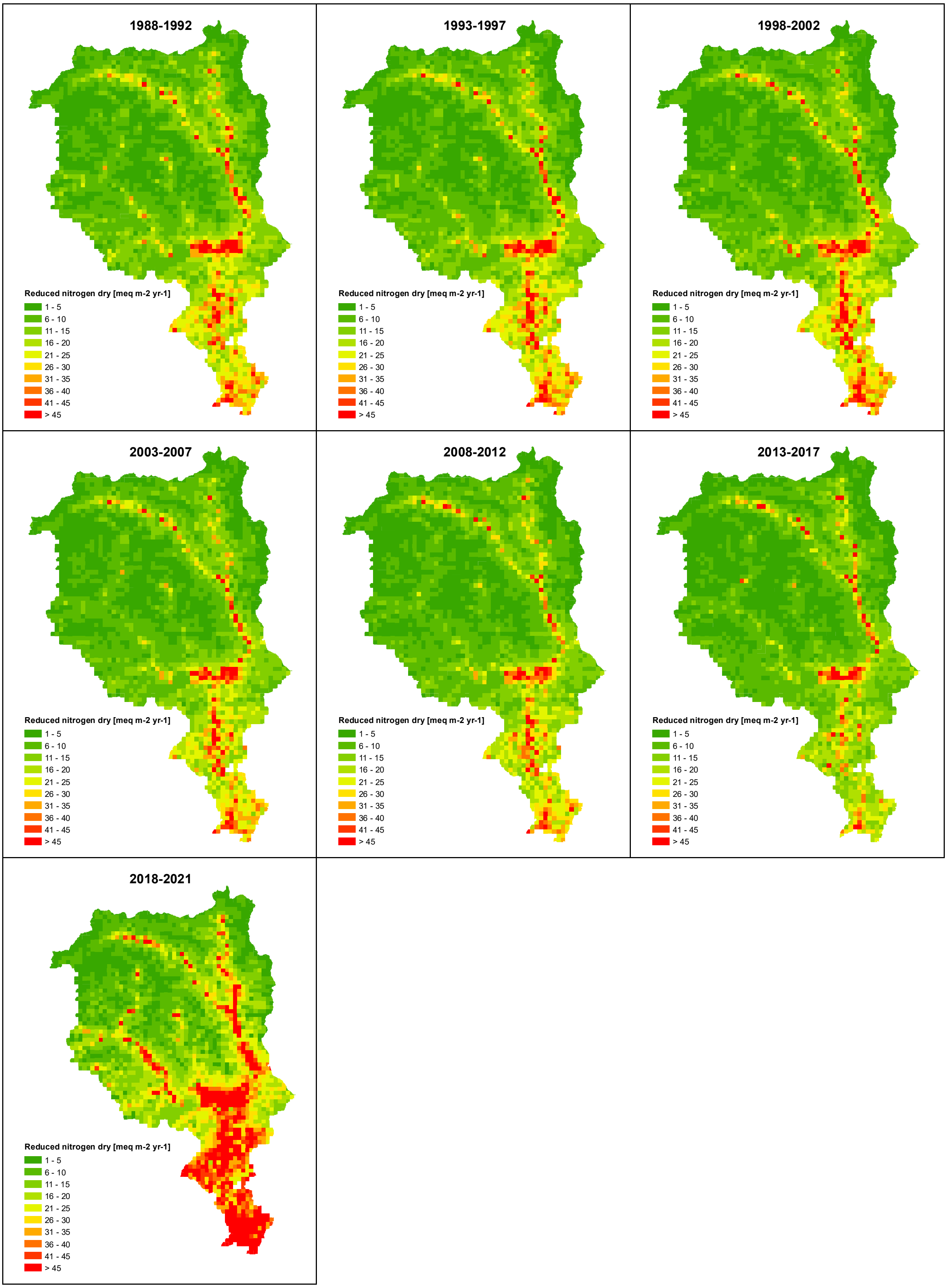

Figure 4.4: Dry deposition of base cations

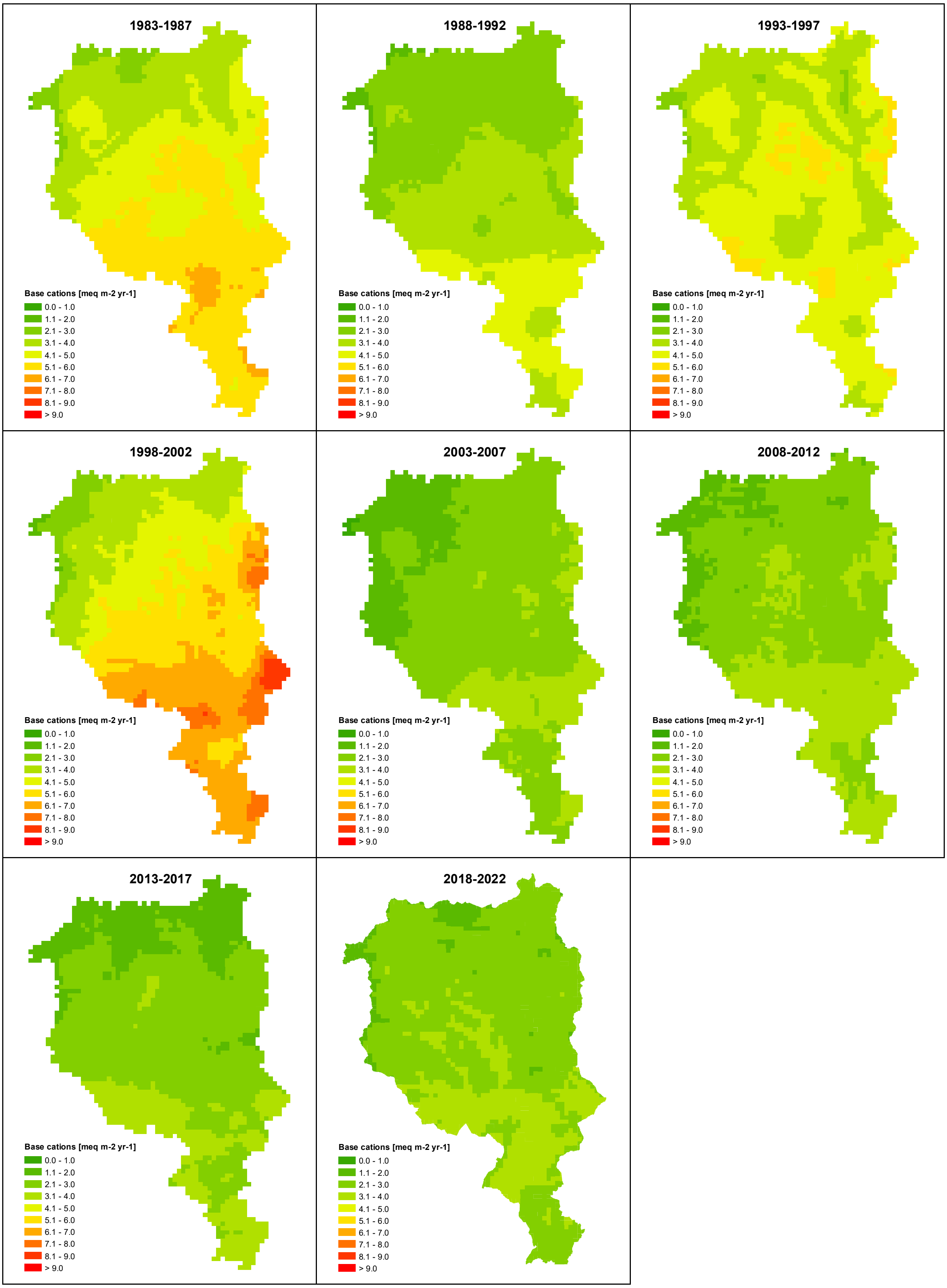

5. Total deposition

5.1 Mapping methods

Fig. 5.1-5.5 illustrate the maps for total deposition of sulphur, oxidized nitrogen, reduced nitrogen, total nitrogen, total base cations and the present load of acidity (PLA). The latter is also known as potential acidity since ammonia is considered as a potential acid.

These maps were produced by adding up the maps of wet and dry depositions discussed in the previous chapters. Since for the period 1983-1987 dry deposition maps were not available, maps of 1988-1992 were used. The total deposition maps were then calculated as follows:

Total sulphur deposition:
wet deposition (SO_4^{2-}) + dry deposition (SO_2)

Total oxidized nitrogen deposition:
wet deposition (NO_3^-) + dry deposition (NO_2 + NO_3^- + HNO_3)

Total reduced nitrogen deposition:
wet deposition (NH_4^+) + dry deposition (NH_3 + NH_4^+)

Total nitrogen deposition:
Total oxidized N + Total reduced N

Total base cations deposition:
wet deposition (BC) + dry deposition (BC)

Present load of acidity (PLA):
Total nitrogen deposition + Total sulphur deposition – Total BC deposition

5.2 Maps

Depositions of total sulphur, total nitrogen and PLA decrease from south to north and from low to high altitude (Fig. 5.1, 5.4, 5.6). Total deposition of sulphur and nitrogen decreased consistently during the monitored period of time. Average total deposition of sulphur and nitrogen decreased from 114 to 22 meq m^{-2} yr^{-1} and from 158 to 114 meq m^{-2} yr^{-1}, respectively. Oxidized and reduced nitrogen contributed with 41% and 59%, respectively to the total. As a consequence of the reduction of sulphur and nitrogen deposition, deposition of the PLA also decreased significantly. Average PLA decreased from 202 to 96 meq m^{-2} yr^{-1}.

Tab. 5.1 presents the relative contribution of wet and dry sulphur and nitrogen deposition to the total acidifying load. Wet deposition contributes most to total deposition of acidifying compounds (between 70% and 79%), depending on the amount of yearly precipitation. Dry deposition is therefore less important. The contribution of sulphur compounds to total deposition of acidifying compounds decreased from 43% to 16%. This is explained by the stronger reduction of sulphur emissions over time compared to that of nitrogen. Accordingly, nitrogen compounds became more important in determining acidifying deposition. In fact, the percentage contribution to total acidifying deposition of reduced and oxidized nitrogen compounds increased from 29% to 35% and from 27% to 49%, respectively.

Figure 5.1: Total deposition of sulphur

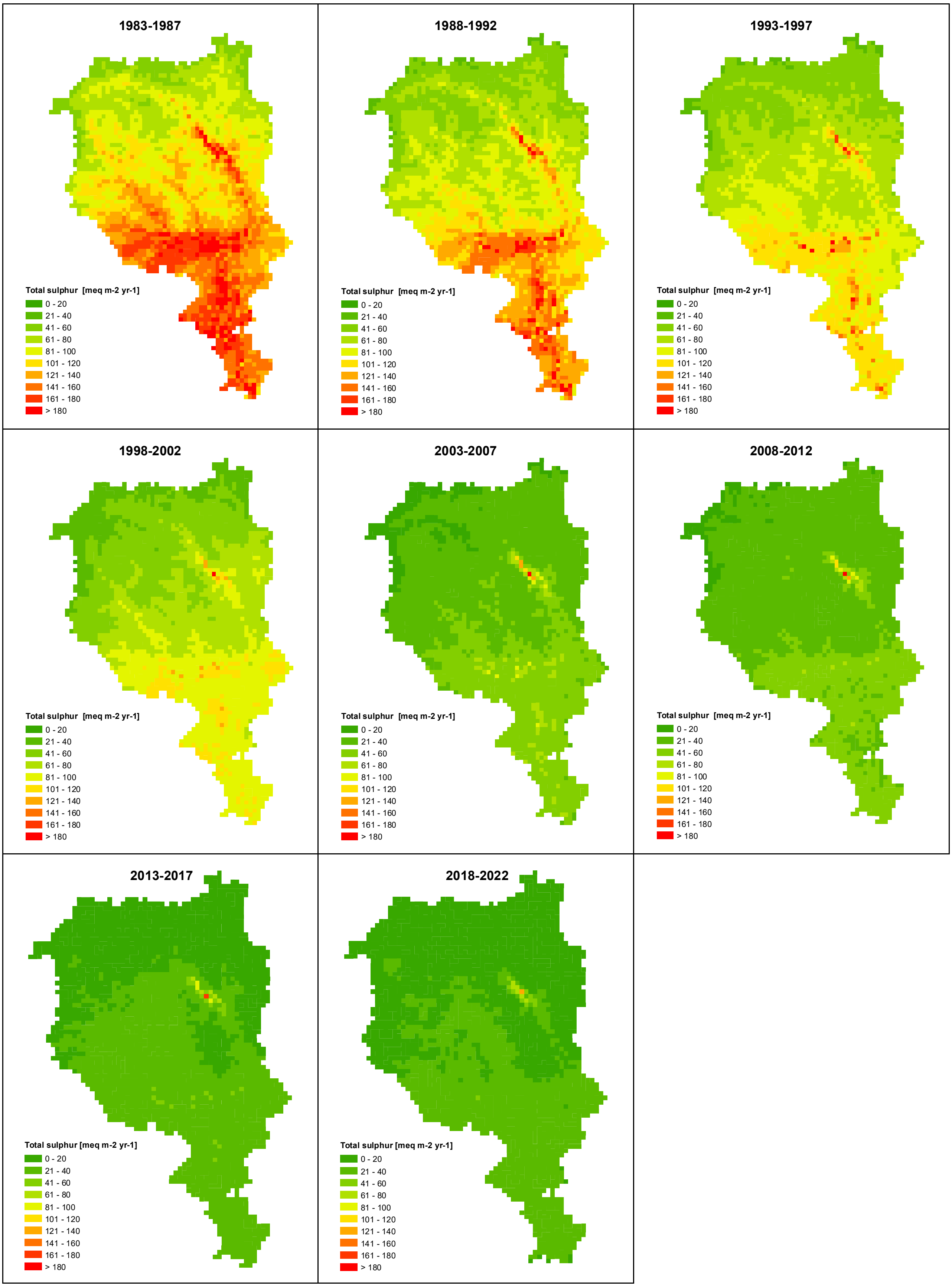

Figure 5.2: Total deposition of oxidized nitrogen

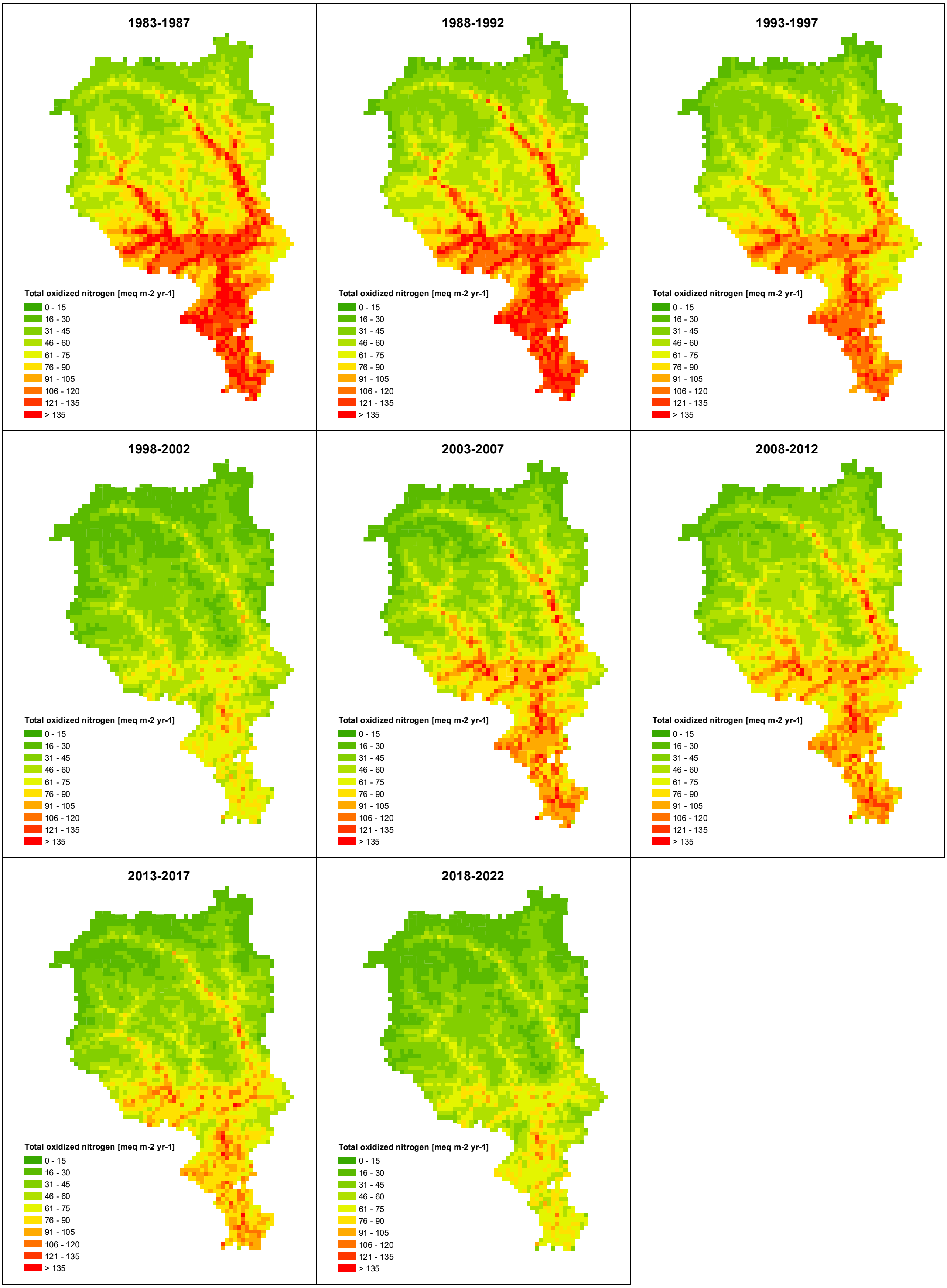

Figure 5.3: Total deposition of reduced nitrogen

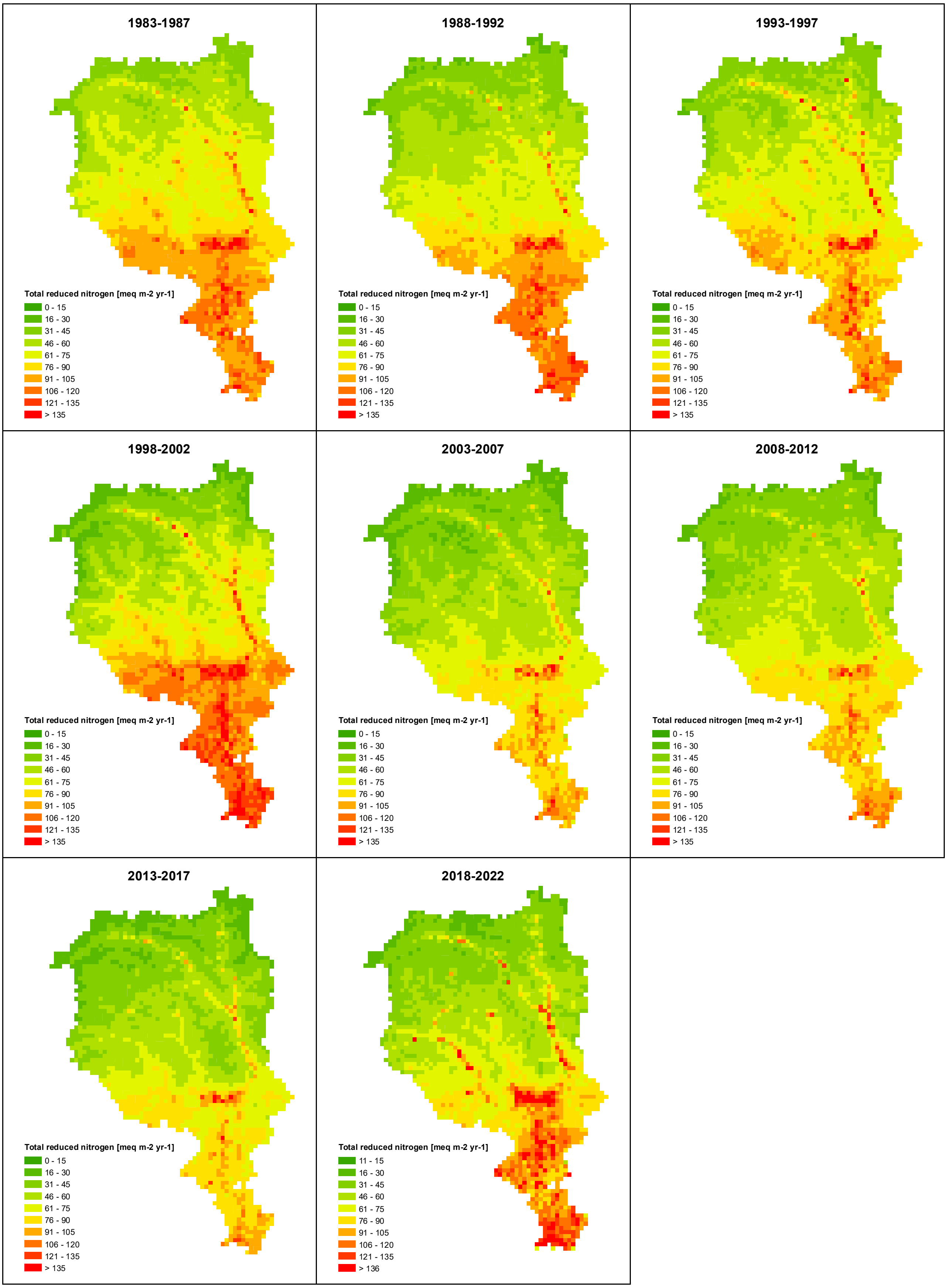

Figure 5.4: Total deposition of nitrogen

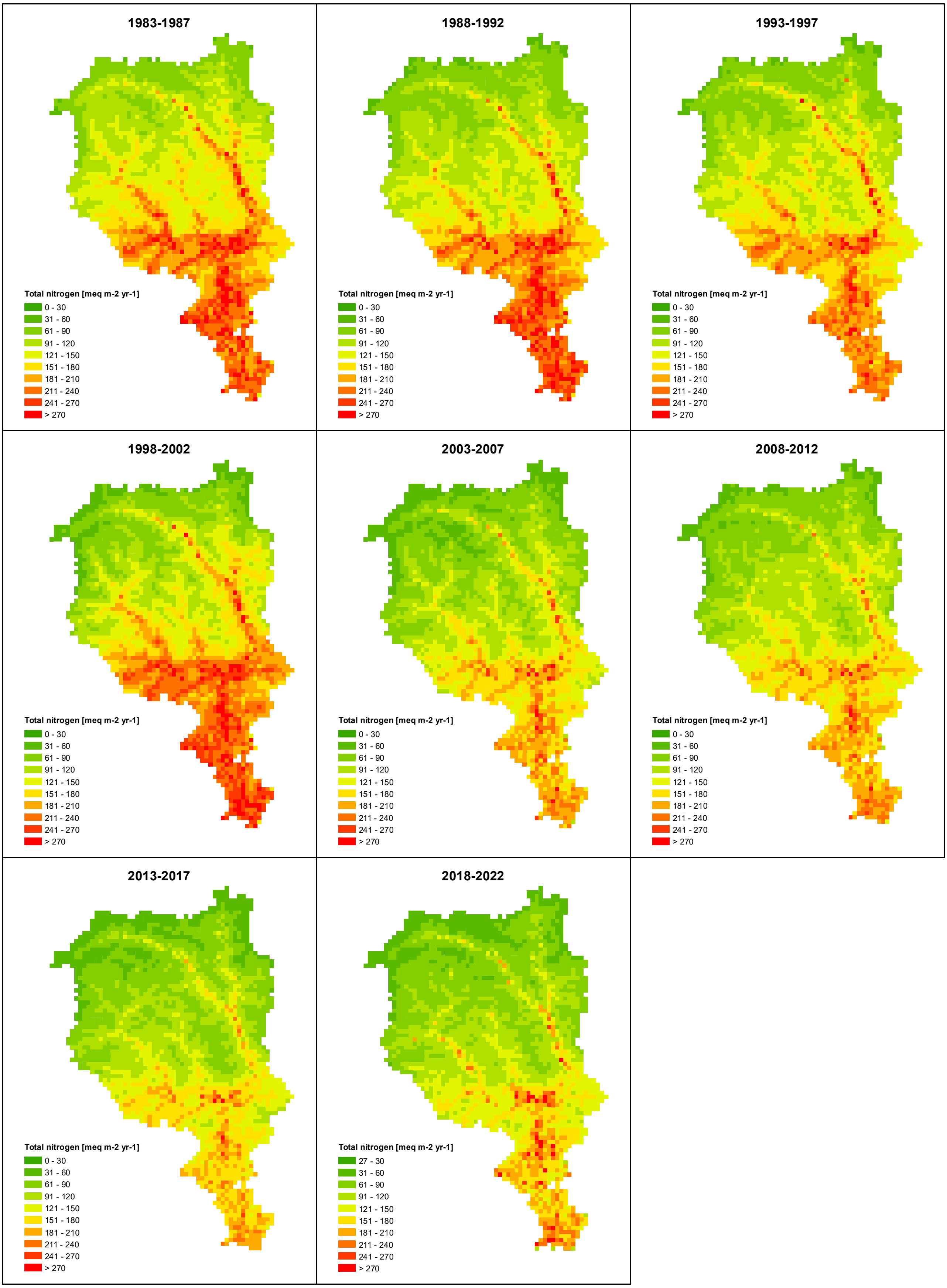

Figure 5.5: Total deposition of base cations

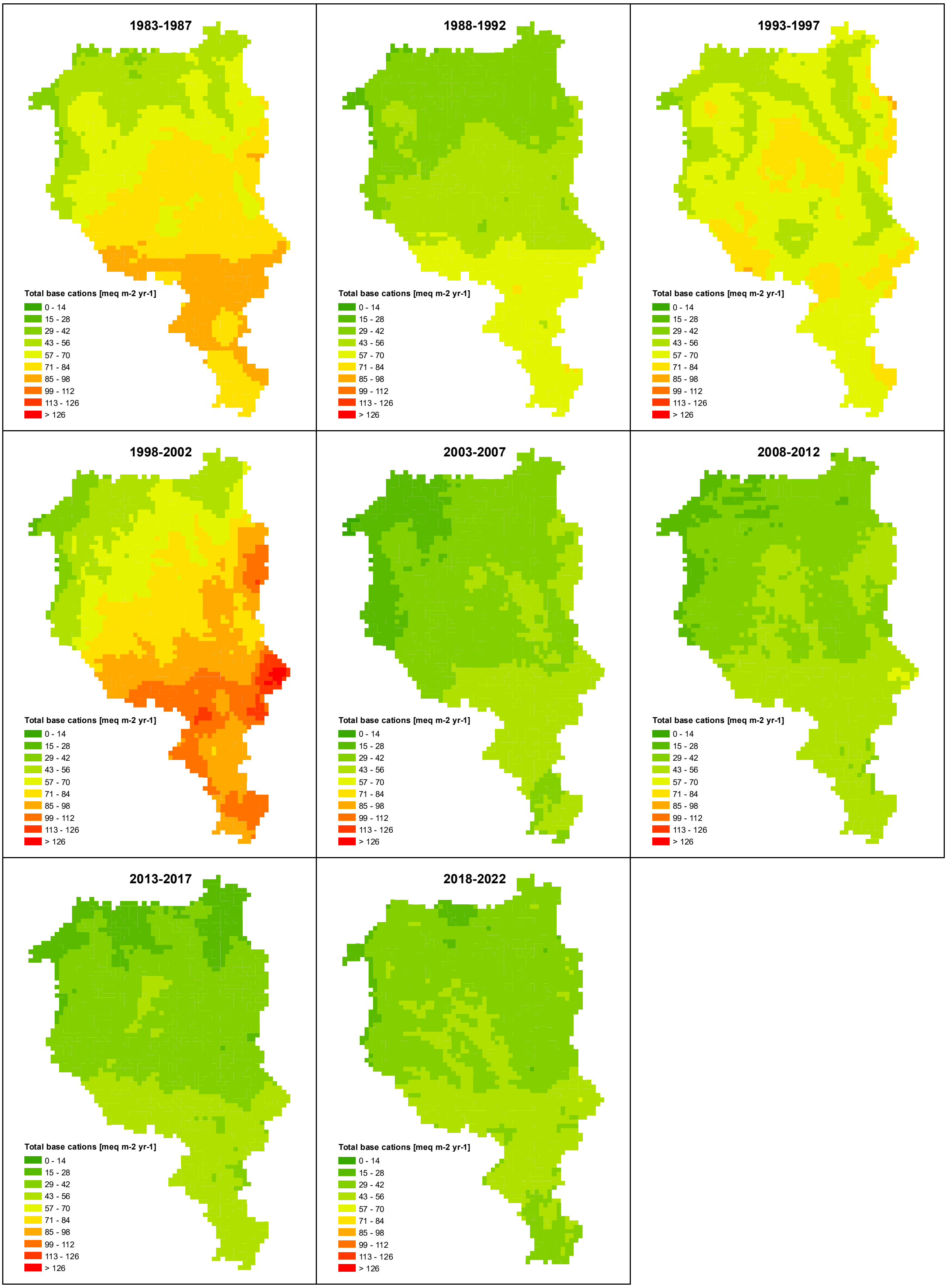

Figure 5.6: Present load of acidity

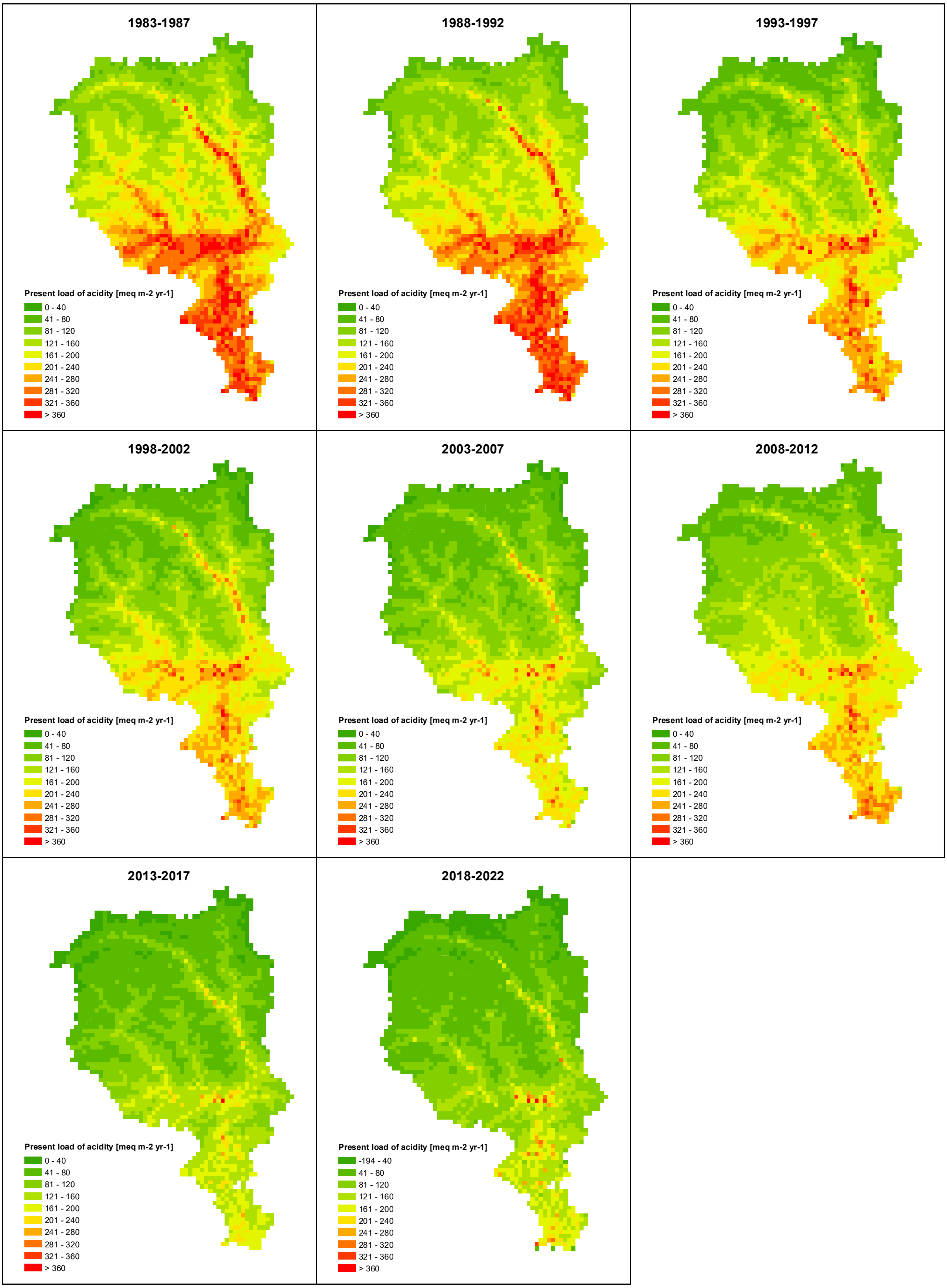

Table 5.1: Relative contribution of wet and dry nitrogen and sulphur deposition to the present load of acidity

Period	Oxidized sulphur		Oxidized nitrogen		Reduced nitrogen	
	wet	dry	wet	dry	wet	dry
1983-1987	35%	8%	20%	9%	23%	5%
1988-1992	30%	9%	21%	11%	24%	5%
1993-1997	30%	7%	21%	11%	25%	6%
1998-2002	29%	3%	24%	10%	28%	5%
2003-2007	20%	5%	25%	14%	29%	7%
2008-2012	20%	3%	26%	13%	31%	7%
2013-2017	16%	3%	26%	14%	34%	7%
2018-2022	14%	2%	22%	13%	34%	16%

References

Austnes et al. 2018. Regional assessment of the current extent of acidification of surface waters in Europe and North America. NIVA report 7268-2018. ICP Waters Report 135/2018. Norwegian Institute for Water Research, Oslo, 134 p.

Barbieri A. and Pozzi S. 2001. Acidifying deposition - Southern Switzerland. Environmental documentation No. 134. Swiss Agency for the Environment, Forests and Landscape, Berne, 113 p.

Bass A.A., Guillevic M., Kegel R., Leuenberger D., Müller B. and Schnker S. 2022. Switzerland's Informative Inventory Report 2022. Submission under the UNCECE Convention on Long-range Transboundary Air Pollution. Federal Office for the Environment, Berne, 434 p.

Dillon P.J., Yan N.D. and Harvey H.H. 1984. Acidic deposition. Effects on aquatic ecosystems. CRC Crit. Rev. Environ. Control 13: 167-194.

EMEP. 2022. Transboundary particulate matter, photo-oxidants, acidifying and eutrophying components. Status Report 1/2022. Norwegian Meteorological Institute, Oslo.

FOEFL. 1994. Critical loads of acidity for forest soils and alpine lakes – steady state mass balance method. Environmental Series Air, 238. Federal Office of Environment, Forests and Landscape, Berne, 68 p.

FOEN. 2023. Nitrogen deposition and exceedances of critical loads for nitrogen in Switzerland 1990-2020. Commissioned by the Federal Office for the Environment, Berne, 106 p.

Gilbert R.O. 1987. Statistical methods for environmental pollution monitoring. John Wiley & Sons, New York, 336 pp.

Grange S.K., Sintermann J. and Hueglin C. (submitted). Sensitivity of atmospheric ammonia (NH_3) trends on meteorology and secondary particulate matter.

Hertz J. and Bucher P. 1990. Abschätzung der totalen Stickstoff- und Protoneneinträge in ausgewählte Ökosysteme der Schweiz. VDI-Berichte 837: 373-387.

Hirsch R.M. and Slack J.R. 1984. A nonparametric test for seasonal data with serial dependance. Water Resources Research 20: 727-732.

Hirsch R.M., Slack J.R. and Smith R.A. 1982. Techniques of trends analysis for monthly water quality data. Wat. Res. Res. 18(1): 107-121.

ICP Waters Programme Centre. 2010. ICP Waters Progamme Manual 2010. NIVA report SNO. 6074-2010. ICP Waters Report 105/2010. Norwegian Institute for Water Research, Oslo, 91 p.

Künzle T. 2022. Karten von Jahreswerten der Luftbelastung in der Schweiz. Datengrundlagen, Berechnungsverfahren und Resultate bis zum Jahr 2021. Im Auftrag des Bundeamtes für Umwelt, Bern, 25 p.

Künzler P. 2005. Weiterentwicklung des Luftreinhalte-Konzepts - Stand, Handlungsbedarf, mögliche Massnahmen. Schriftenreihe Umwelt Nr. 379. Bundesamt für Umwelt, Wald und Landschaft, Bern, 171 p.

Odén S. 1968. The acidification of air and precipitation and its consequences on the natural environment. Ecology Committee, Bulletin No. 1. Swedish National Science Research Council, Stockholm, 117 p.

Marchetto A. 2014. rkt: Mann-Kendall test, Seasonal and Regional Kendall Tests. (ultimo aggiornamento 22.1.2014).

MeteoSvizzera. 2012. Rapporto sul clima – Cantone Ticino 2012. Rapporto di lavoro MeteoSvizzera no. 239, Ufficio federale di meteorologia MeteoSvizzera, Locarno Monti, 63 p.

Rogora M., Colombo L., Lepori F., Marchetto A., Steingruber S. and Tornimbeni O. 2013. Thirty Years of Chemical Changes in Alpine Acid-Sensitive Lakes in the Alps. Water Air Soil. Pollut. 29(41): 62312–62329.

Rogora M., Colombo L., Marchetto A., Mosello R. and Steingruber S. (2016). Temporal and spatial patters in the chemistry of wet deposition in Southern Alps. Atmos. Environ. 224(10): 1746

Rogora M., Steingruber S., Marchetto A., Mosello R., Giacomotti P., Orru A., Tartari G.A. and Tiberti R. (2022) Response of atmospheric deposition and surface water chemistry to the COVID-19 lockdown in an alpine area. Environ. Sci. Pollut. Res. 29: 62312-62329.

Seitler E. and Meier M. 2022. Ammoniak-Immissionsmessungen in der Schweiz 2000 bis 2021, Messbericht. Forschungsstelle für Umweltbeobachtung (FUB). Im Auftrag des Bundesamtes für Umwelt (BAFU), der OSTLUFT (AI, AR, GL, GR, SG, SH, TG, ZH, FL), der inNET (LU, NW, OW, SZ, UR, ZG), und der Kantone AG, BE, BL/BS, FR, NE, SO. Forschungsstelle für Umweltbeobachtung, Rapperswil,, 79 p. (https://www.bafu.admin.ch/bafu/de/home/themen/luft/publikationen-studien/studien.html)

Smith R.A. 1852. On the air and rain of Manchester. Memoirs of the Manchester Literary and Philosophical Society 10: 207-217.

Spinedi F. and Isotta F.. 2004. Il clima del Ticino. Dati - statistiche e società 2: 4-39.

Steingruber S. 2018. Acidifying deposition in Southern Switzerland – Monitoring, maps and trends 1983-2017. Dipartimento del territorio del Canton Ticino, Bellinzona, 54 p.

Steingruber S. 2023. Results from the participation of Switzerland to the International Cooperative Programme on Assessment and Monitoring Effects of Air Pollution on Rivers and Lakes (ICP Waters). Biannual report 2021-2022. Dipartimento del territorio del Canton Ticino, Bellinzona, 82 p.

Steingruber S. and Colombo L. 2010. Acidifying deposition in Southern Switzerland - Assessment of the trend 1988-2007. Environmental studies no. 1015, Federal Office for the Environment, Bern, 82 p.

Acknowledgments

The study was financially supported by the Federal Office for the Environment (FOEN).

We would also like to thank the Institute of Ecosystem Study (Verbania Pallanza, Italy) for supplying their wet deposition monitoring data and Beat Rihm (Meteotest, Bern) for preparing and forwarding national dry deposition maps.

We are also grateful to Giovanni Kappenberger for yearly winter snow sampling at the glacier Basodino, the laboratory of the Section for air, water and soil protection of the Department of the territory of the Canton of Ticino for chemical analyses and all those that over the years sampled and submitted rainwater at weakly intervals for the analysis.

Appendix

Table A1: Swiss (CH) and Italian (I) precipitation sampling sites and their Swiss coordinates (CH1903 LV03), altitudes, data source and period used for the calculation of the depositions during 2018-2022

N°	Sampling site	Country	Longitude (m)	Latitude (m)	Altitude (m a.s.l.)	Date source
1	Agrasina	Italy	674587	119675	1370	Idroelettriche Riunite S.p.A.
2	Arcisate	Italy	712824	78131	383	ARPA Lombardia
3	Bruggi	Italy	676295	133657	1226	ARPA Piemonte
4	Lago Morasco	Italy	673975	142207	1820	ENEL
5	Lago Sabbione	Italy	670084	141680	2462	ENEL
6	Lago Toggia	Italy	676351	143398	2200	ENEL
7	Lago Truzzo	Italy	744807	136010	2064	ARPA Lombardia
8	Lavena Ponte Tresa	Italy	710314	91714	279	ARPA Lombardia
9	Luino	Italy	701193	94821	205	ARPA Lombardia
10	Piano dei Camosci	Italy	670990	143013	2450	ARPA Piemonte
11	Acquarossa/Comprovasco	Switzerland	714998	146440	575	MeteoSwiss
12	Airolo	Switzerland	688910	153400	1138	MeteoSwiss
13	Andermatt	Switzerland	687444	165044	1438	MeteoSwiss
14	Bellinzona	Switzerland	720913	116588	224	MeteoSwiss
15	Biasca	Switzerland	718550	132800	278	MeteoSwiss
16	Bosco Gurin	Switzerland	680879	130027	1486	MeteoSwiss
17	Braggio	Switzerland	729975	128600	1315	MeteoSwiss
18	Brissago	Switzerland	698200	108390	280	MeteoSwiss
19	Camedo	Switzerland	690296	112207	590	MeteoSwiss
20	Cevio	Switzerland	689688	130565	417	MeteoSwiss
21	Cimetta	Switzerland	704433	117452	1661	MeteoSwiss
22	Coldrerio	Switzerland	721080	79235	347	MeteoSwiss
23	Crana-Torricella	Switzerland	712695	103746	1002	MeteoSwiss
24	Disentis/Sedrun	Switzerland	708189	173789	1197	MeteoSwiss
25	Faido	Switzerland	704950	148266	747	MeteoSwiss
26	Göschenen	Switzerland	688477	171926	950	MeteoSwiss
27	Göscheneralp	Switzerland	681250	166790	1745	MeteoSwiss
28	Grimsel Hospiz	Switzerland	668583	158215	1980	MeteoSwiss
29	Grono	Switzerland	733017	124090	324	MeteoSwiss
30	Gütsch ob Andermatt	Switzerland	690050	167475	2287	MeteoSwiss
31	Hinterrhein	Switzerland	733900	153980	1611	MeteoSwiss
32	Locarno Monti	Switzerland	704160	114350	367	MeteoSwiss
33	Lugano	Switzerland	717874	95884	273	MeteoSwiss
34	Magadino/Cadenazzo	Switzerland	715475	113162	203	MeteoSwiss
35	Mesocco	Switzerland	737850	139825	830	MeteoSwiss
36	Monte Generoso	Switzerland	722503	87456	1600	MeteoSwiss
37	Morbio Superior	Switzerland	722750	80075	440	MeteoSwiss
38	Mosogno	Switzerland	692803	117050	771	MeteoSwiss
39	Olivone	Switzerland	715465	154865	958	MeteoSwiss
40	Piotta	Switzerland	695888	152261	990	MeteoSwiss
41	Ponte Tresa	Switzerland	710110	91630	274	MeteoSwiss
42	Robiei	Switzerland	682588	144091	1896	MeteoSwiss
43	S. Bernardino	Switzerland	734112	147296	1639	MeteoSwiss
44	Scudellate	Switzerland	724175	86850	925	MeteoSwiss
45	Sedrun	Switzerland	699974	169845	1429	MeteoSwiss
46	Sonogno	Switzerland	703822	134052	912	MeteoSwiss
47	Splügen	Switzerland	744420	157435	1460	MeteoSwiss
48	Stabio	Switzerland	716050	77966	353	MeteoSwiss

N°	Sampling site	Country	Longitude (m)	Latitude (m)	Altitude (m a.s.l.)	Date source
49	Ulrichen	Switzerland	666740	150760	1346	MeteoSwiss
50	Vals	Switzerland	734016	165552	1278	MeteoSwiss
51	Vira Gambarogno	Switzerland	709400	111680	199	MeteoSwiss
52	Vrin	Switzerland	727220	168526	1384	MeteoSwiss
53	Zervreila	Switzerland	728780	160000	1738	MeteoSwiss
54	Alpe di Neggia	Switzerland	708764	107528	1395	UCA
55	Arosio	Switzerland	713130	100610	660	UCA
56	Bedretto	Switzerland	682303	151023	1397	UCA
57	Biasca	Switzerland	717000	135125	293	UCA
58	Biasca Pontirone	Switzerland	723860	137864	1405	UCA
59	Cabbio	Switzerland	724643	84028	612	UCA
60	Camedo	Switzerland	690050	112110	558	UCA
61	Campo Vallemaggia	Switzerland	681711	126785	1303	UCA
62	Carena	Switzerland	727230	114230	942	UCA
63	Cavergno	Switzerland	690081	133073	455	UCA
64	Chiasso	Switzerland	722690	77090	240	UCA
65	Colla	Switzerland	725030	106400	1140	UCA
66	Fusio	Switzerland	694115	144405	1276	UCA
67	Giubiasco	Switzerland	719712	114774	215	UCA
68	Gnosca (CH)	Switzerland	721880	122072	247	UCA
69	Grancia (CH) (CH)	Switzerland	715328	92408	310	UCA
70	Isone (CH)	Switzerland	720176	110336	792	UCA
71	Lavertezzo (Aquino)	Switzerland	707124	124609	635	UCA
72	Maggia (CH)	Switzerland	697620	122190	316	UCA
73	Mendrisio (CH)	Switzerland	719211	82996	290	UCA
74	Novaggio (CH)	Switzerland	709980	96160	620	UCA
75	Olivone (CH)	Switzerland	715410	154120	909	UCA
76	Olivone Luzzone Diga (CH)	Switzerland	716665	158232	1612	UCA
77	Piora	Switzerland	697970	155860	1964	UCA
78	Sonogno (CH)	Switzerland	703633	133902	913	UCA

Table A2: Mean annual rainwater concentrations at the Swiss wet deposition sampling sites from 2018 to 2022. Prec and Cond correspond to precipitation and conductivity, respectively. * NO_3 estimated from Devero (Italy) and GranAlk from ANC

Year	Prec	Analysed Prec	Cond 20°C	pH	Ca	Mg	Na	K	NH_4	NO_3	SO_4	Cl	GranAlk
	mm	%	$\mu S\ cm^{-1}$		meq m^{-3}								
Acquarossa													
2018	1077	100	8	5.7	23	3	6	2	28	19	13	6	26
2019	1393	96	9	5.8	24	4	5	3	38	21	16	6	33
2020	1097	95	5	5.7	12	2	4	1	19	12	7	4	14
2021	1121	82	8	5.8	28	4	4	2	32	18	12	4	32
2022	636	98	8	6.1	19	3	5	2	42	20	12	4	24
Bignasco													
2018	1869	95	9	5.6	21	4	8	2	29	25	14	9	22
2019	2271	90	9	5.7	26	4	6	2	31	31	15	5	29
2020	1558	90	6	5.7	16	5	6	3	19	18	9	6	17
2021	1493	84	9	5.8	36	4	7	3	33	35	14	7	34
2022	846	82	10	6.2	20	3	6	3	51	36	13	6	36
Monte Brè													
2018	1474	79	12	5.9	35	8	12	4	40	33	20	12	36
2019	1675	93	9	5.6	20	3	9	2	32	24	15	9	20
2020	1543	66	7	5.7	14	3	6	1	27	17	8	7	19
2021	1444	90	7	5.9	22	4	7	2	29	19	12	7	21
2022	1096	92	11	6.1	20	4	9	4	56	26	14	8	40
Cristallina													
2019			7	5.7	17	2	6	3	29	18	11	6	17
2021			5	5.6	13	2	2	1	19	10	13	3	12
2022			6	6.0	14	2	3	1	32	16	9	3	23
Locarno Monti													
2018	1467	91	10	5.6	25	5	10	2	32	25	17	10	23
2019	1868	93	8	5.5	17	4	7	2	28	20	14	6	17
2020	1599	90	6	5.7	14	3	7	1	25	15	10	6	17
2021	1612	82	9	5.8	23	4	7	2	40	23	15	7	26
2022	1283	91	9	6.0	14	3	8	1	53	23	14	7	32
Lugano													
2018	1474	50	11	6.1	35	5	8	3	43	43	18	9	42
2019	1675	81	10	5.5	21	4	7	2	40	40	17	8	24
2020	1543	81	8	5.8	21	4	6	2	36	36	11	7	28
2021	1444	80	8	5.6	21	4	7	2	34	34	13	8	20
2022	1096	79	12	6.2	21	5	9	2	67	67	16	9	44
Piotta													
2018	1616	85	7	5.7	23	3	9	1	19	15	12	9	19
2019	1843	87	8	5.8	24	2	9	1	25	16	13	9	25
2020	1306	87	12	5.8	14	2	73	1	14	12	7	70	11
2021	1302	80	9	5.9	30	3	20	1	29	16	11	21	32
2022	895	87	9	6.1	26	3	8	1	37	16	12	8	38
Robiei*													
2018	2665	75			15	3	4	1	17	13	12	5	12
2019	3070	71			17	2	3	2	18	14	10	4	14
2020	1981	69			11	2	4	1	10	9	6	3	9
2021	2352	83			18	3	5	2	25	14	11	3	24
2022	1541	86			16	3	3	1	20	16	10	3	14
Sonogno													
2018	1867	69	9	6.0	17	3	8	3	44	24	14	8	29
2019	2326	92	7	5.8	18	2	4	1	28	18	12	4	22
2020	1800	80	5	5.7	11	2	3	1	20	13	7	3	14
2021	1832	84	9	5.9	34	4	5	2	37	19	12	5	41
2022	1270	76	8	6.0	14	3	4	1	43	20	11	4	29

Year	Prec	Analysed Prec	Cond 20°C	pH	Ca	Mg	Na	K	NH_4	NO_3	SO_4	Cl	GranAlk
	mm	%	µS cm^{-1}		meq m^{-3}								
Stabio													
2018	1489	90	11	5.7	23	4	3	9	46	32	17	9	29
2019	1542	84	11	5.5	22	6	4	12	46	31	17	12	28
2020	1350	92	10	5.8	26	5	2	9	44	22	12	9	39
2021	1540	91	9	5.8	21	4	2	8	43	24	14	8	27
2022	794	88	11	6.0	17	5	4	8	60	27	13	8	38

Table A3: Average concentrations in rainwater in the periods of 2018-2022 used for the correlation analysis. Prec corresponds to precipitation. * estimated from Devero

Period	Prec	SO_4	NO_3	NH_4	Ca+Mg+K
	mm	meq m^{-3}			
Acquarossa	1065	12	18	31	27
Bignasco	1607	13	20	9	30
Monte Brè	1446	14	24	36	29
Cristallina	2113	10	15	25	14
Locarno Monti	1566	14	21	35	24
Lugano	1446	15	24	43	30
Piotta	1393	11	15	24	27
Robiei	2322	10	13*	18	19
Sonogno	1819	11	18	34	24
Stabio	1343	15	27	47	30
Devero	1646	9	13	22	18
Domodossola	1283	12	18	37	27
Pallanza	1614	15	25	46	23
Basodino	1764	7	7	9	13

Table A4: Results from multiple regression analysis for 2018-2022. n, r^2, F, p stay for data number, coefficient of determination, F statistic and p-values.

Period	n	r^2	F	p	m_{lat} meq m^{-4}	m_{long} meq m^{-4}	m_{alt} meq m^{-4}	C_0 meq m^{-3}
Ca+Mg+K	14	0.79	17.5	0.000	2.0E-5	9.3E-5	-5.3E-3	-37.7
NH_4	14	0.58	7.0	0.008	-2.9E-4	1.1E-4	-3.1E-3	-9.2
SO_4	14	0.89	37.3	0.000	-3.3E-5	3.3E-5	-1.5E-3	-5.2
NO_3	14	0.89	36.7	0.000	-1.1E-4	8.6E-5	-2.5E-3	-25.6